# CALCULATION SUMMARY SHEET



PROJECT NUMBER: 143418

PROJECT NAME: USEN – Trench 13 Design

DATE: January 20, 2015

CALCULATION NUMBER: C.09 Revision: 1 (March 11, 2016)

**CALCULATION TITLE: Liner Stability on Trench 13 Side-Slopes**

**DESCRIPTION OF CALCULATION:**

Evaluate the tension/elongation of the design slope liner system to prevent ruptures or damage to the liner system due to gravity, thermal expansion/contraction, wind uplift, seismic deformation, and waste settlement.

**REFERENCES USED:**

1. Technical Journals for Interpretation of Friction Angles of Geosynthetics
2. Koerner, “Designing with Geosynthetics” 1998.
3. Trench 12 Liner Material Properties – Used as basis for stability evaluation.

**REVIEW COMMENTS:**

.

| | | | |
|---|---|---|---|
| CALCULATION MADE BY: | CWK | DATE: | 01/20/15 |
| CALCULATION CHECKED BY: | PAZ | DATE: | 04/24/15 |
| CALCULATION REVISED BY: | CWK | DATE: | 04/29/15 |
| CALCULATION REVIEWED BY: | CAB | DATE: | 04/29/15 |

# CALCULATION
# LINER STABILITY – TRENCH 13 SIDE SLOPES

## PURPOSE OF CALCULATION

Determine the stability of liner materials on Trench 13 0.5H:1.0V (604/29/153.4°) slopes. Stability in this calculation refers to liner material strength and capacity to remain intact and functional under the loads that will be imposed by liner material weight (self-weight of liner members and loading from overlying liner members) and resistance of liner due to friction.

## METHOD

The following causes of liner stresses are considered:

- Load due to gravity
- Thermal expansion and contraction
- Wind uplift
- Seismic deformation
- Settlement of waste fill

### General

This calculation analyzes strength for liner materials proposed for use in Trench 13 at US Ecology's Beatty, Nevada facility. Stresses and strains on liner materials are estimated from the self-weight of the liners, thermal expansion, seismic deformation, and settlement of the waste fill. The total induced stress from these factors is compared to estimated allowable stresses on the liner materials from estimated factors of safety.

Material properties for all members of the Trench 13 liner system are taken from manufacture specifications for products approved for use in US Ecology's Trench 12 design. This calculation evaluates those material properties as they pertain to the design of US Ecology's Trench 13.

The liner materials will be placed on a 0.5H:1.0V slope (an angle of 63.4° below horizontal). The trench will have a maximum depth of approximately 75 feet resulting in a slope length of 84 feet.

$$Slope\ Length = \frac{75\ ft}{\sin(63.4°)} = 84\ ft$$

## Self-Weight Forces on Liner Members and Tensile Loads

Assuming stable slopes, the load due to gravity (tensile load) on the liners is due to self-weight (shown in Table 1 below). The weight on the liner members accumulates for underlying liner members.

Self-weight = Unit Weight * Slope Length

Self-weight is the length of liner member (slope length = 84 feet) times the unit weight of the liner material, which is expressed in lbs per foot. The unit weight of each liner material was obtained from specification sheets from liner member manufacturers. Table 1 gives the unit weight from the manufacturer, the self-weight determined from the slope length of 84 feet for the design liner materials, and the accumulated weight for underlying liner members.

**Table 1: Accumulated Weight of Liner System**

| Liner Material (reference for product data) | Unit Weight (lbs/ft^2) | Self-weight (lbs/ft) | Accumulated Weight (lbs/ft) |
|---|---|---|---|
| Sacrificial 40 Mil HDPE Liner | 0.20 | 16 | 16 |
| 10oz Non-woven Geotextile | 0.069 | 5.8 | 22 |
| Geonet – LCRS Side Slope – 200 Mil | 0.162 | 14 | 36 |
| 80 Mil HDPE Single Sided Texture | 0.37 | 31 | 67 |
| LDS Side Slope Geocomposite 6 oz double-sided 200 Mil | 0.25 | 21 | 88 |
| 60 Mil HDPE Double Sided Texture | 0.28 | 23 | 111 |
| Geosynthetic Clay Liner | 0.75 | 63 | 174 |

*Note: Unit weights are based upon manufacture specifications*
*Manufacturer specifications for 200 Mil Geonet and 200 Mil Geocomposite are the same as 220 Mil manufacturer specifications included in References.*

## Frictional Forces Acting on the Trench 13 Liner System

Friction forces acting on the upper side ($F_U$) of the liner and the forces acting on the lower side ($F_L$) of the liner were calculated using free body diagram analysis. $F_U$ equals the friction force acting on the upper side of the liner member. This friction ($F_U$) is part of the total force that is tending to cause liner member failure. $F_L$ is the component of the resultant force that resists failure as shown in **Figure 1**.

$F_L$ = AW * cos(B) * tan(d)
$F_U$ =$F_L$ of liner component above

Where:
AW = accumulated weight of liner members
d = friction angle between liner components
B = slope angle (i.e. 63.4° below horizontal)

Accumulated weight (AW) is tabulated in Table 1. Slope angle (B) is the angle of the slope (63.4°). Friction angle (d) is the residual friction angle which is dependent on the liner materials that are in contact with each other. A graphical representation of the liner

members with frictional forces is attached as **Figure 2**. The tensile load due to self-weight (T) is calculated:

$$T = ((SW * \sin(B)) + F_U - F_L)/(12inch/1foot)$$

Where:

SW = self-weight of liner members

The friction forces and tensile load for each liner member are calculated in Table 2. The residual friction angles were obtained from technical documents provided by manufactures as well as direct shear tests of geosynthetics performed and reported in multiple journals and technical literature.

**Table 2: Tensile Load due to Frictional Forces of Liner Members**

| Material | Self Weight *lb/ft* | Accumulated Weight *lb/ft* | Friction Angle Theta Θ | Reference # | Friction Upper Fu *lb/ft* | Friction Lower Fl *lb/ft* | Tensile Load *lb/in* |
|---|---|---|---|---|---|---|---|
| Sacrificial 40 Mil HDPE Liner | 16 | 16 | 15.1 | 1-A | 0.0 | 2.0 | 1.1 |
| 10oz Non-woven Geotextile | 5.8 | 22 | 24.5 | 1-B | 2.0 | 4.5 | 0.22 |
| Geonet – LCRS Side Slope – 200 Mil | 14 | 36 | 10.1 | 1-B | 4.5 | 2.9 | 1.2 |
| 80 Mil HDPE Single Sided Texture | 31 | 67 | 32.1 | 1-C | 2.9 | 19 | 1.0 |
| LDS Side Slope Geocomposite 6 oz double-sided 200 Mil | 21 | 88 | 32.1 | 1-C | 18.8 | 25 | 1.1 |
| 60 Mil HDPE Double Sided Texture | 23 | 111 | 24 | 1-D | 25 | 22 | 2.0 |
| Geosynthetic Clay Liner | 63 | 174 | 21.6 | 1-E | 22 | 31 | 4.0 |

**Note:** See attached references for description of friction angle determination

## Summary of Liner Member Strengths and Strains

The following table summarizes the tensile strength at yield and percent strain at yield for each liner member. The tensile strength at yield is the strain at which the liner member deforms. Prior to the yield point the material will deform elastically and will return to its original shape when the applied stress is removed. The amount of elongation at yield also is known as the strain at yield and is reported as a percent. The information below was obtained from material specification sheets provided by the manufacturers.

**Table 3: Yield Strength and Strain of Liner Members**

| Liner Material | Yield Strength (lb/in) | Strain (elongation) at Yield % |
|---|---|---|
| Sacrificial 40 Mil HDPE Liner | 84 | 12 |
| 10oz Non-woven Geotextile | 150* | 50 |
| Geonet – LCRS Side Slope – 200 Mil | 45 | 23* |
| 80 Mil HDPE Single Sided Texture | 176 | 13 |
| LDS Side Slope Geocomposite 6 oz double-sided 200 Mil | 50 | 50 |
| 60 Mil HDPE Double Sided Texture | 132 | 13 |
| Geosynthetic Clay Liner | 50 | 15* |

*Values taken from Koerner 1998 – Designing with Geosynthetics – **Reference 2**

## Calculation of Strains

Four strains are considered on the liner members including strain due to 1) tensile load from frictional forces, 2) thermal expansion, 3) seismic deformation, 4) settlement of waste fill. The calculation of each strain is described below.

Strain due to tensile load from frictional forces is calculated by comparing the percent strain at yield of each member to the tensile load due to frictional forces. For example:

(Tensile load due to friction force (lbs/in))/(Yield strength of liner member (lbs/in)) = (Strain due to frictional forces(%))/(Strain at yield of liner member (%)) where strain due to frictional forces is the unknown.

Rearranging the equation:
Strain due to frictional forces (%) = Tensile load due to frictional forces (lbs/in)/Yield Strength of liner member (lbs/in)*Strain at yield (%).

Example using the 60-Mil HDPE where

Tensile load due to frictional force = 2.0 lbs./in
Yield Strength = 132 lbs./in
Strain at yield = 13%

Therefore, Strain due to frictional forces for the 60-Mil HDPE =

$$\frac{2.0 lbs./in}{132 lbs./in} * 13\% = 0.20\%$$

**Table 4: Strain due to Self-weight on Liner Members**

| Material | Tensile Load (due to frictional forces) *lb/in* | Yield Strength *(lb/in)* | Strain at Yield *%* | Strain due to frictional forces *%* |
|---|---|---|---|---|
| Sacrificial 40 Mil HDPE Liner | 1.06 | 84 | 12 | 0.15 |
| 10oz Non-woven Geotextile | 0.22 | 150 | 50 | 0.074 |
| Geonet – LCRS Side Slope – 200 Mil | 1.2 | 45 | 23 | 0.59 |
| 80 Mil HDPE Single Sided Texture | 1.0 | 176 | 13 | 0.073 |
| LDS Side Slope Geocomposite 6 oz double-sided 200 Mil | 1.1 | 50 | 50 | 1.1 |
| 60 Mil HDPE Double Sided Texture | 2.0 | 132 | 13 | 0.19 |
| Geosynthetic Clay Liner | 4.0 | 50 | 15 | 1.2 |

Strain due to thermal expansion is considered only for HDPE Geomembranes and Geonets. From a conversation with a liner technical representative, the coefficient of linear thermal expansion is 0.00012 cm/cm*°C (ESI 1996). An assumption for temperature variation is 40°C for the purposes of this calculation. Therefore; the strain due to thermal expansion is 0.00012 cm/cm*°C * 40°C, or 0.5%.

Seismic deformation during waste placement is expected to be small, less than 1.6 inches (ESI 1996), considered on a slope length of 84 feet, 1.6 inches equates to approximately 0.2%. This strain will only act on the first two liner members because the liner system is designed to allow slippage between the third and fourth liner members (Geonet and 80-Mil HDPE) and seismic strain is not expected to be transferred below that interface.

Strain from waste fill settlement also was considered. 1996 Trench 12 Design documents (ESI 1996)[1] estimated the strain from waste fill settlement is no greater than 4%, including settlement during waste placement and after closure of the landfill. Strain due to waste settlement will again only act on the first two liner members because of the design slippage between the second and third liner members.

1. 1996 Trench 12 Design Documents are discussed multiple times in this calculation, however are not attached to this specific calculation. The 1996 Trench 12 Design Documents will be attached as a separate document and submitted with the design report.

**Table 5: Total Strain on Liner Members**

| Material | Strain due to frictional forces % | Strain - Thermal Expansion % | Strain - Seismic Deformation % | Strain - Waste Settlement % | Total Strain % |
|---|---|---|---|---|---|
| Sacrificial 40 Mil HDPE Liner | 0.15 | 0.5 | 0.2 | 4.0 | 4.9 |
| 10oz Non-woven Geotextile | 0.074 | 0 | 0.2 | 4.0 | 4.3 |
| Geonet – LCRS Side Slope – 200 Mil | 0.59 | 0.5 | 0.2 | 4.0 | 5.3 |
| 80 Mil HDPE Single Sided Texture | 0.073 | 0.5 | 0 | 0 | 0.57 |
| LDS Side Slope Geocomposite 6 oz double-sided 200 Mil | 1.1 | 0 | 0 | 0 | 1.1 |
| 60 Mil HDPE Double Sided Texture | 0.19 | 0.5 | 0 | 0 | 0.69 |
| Geosynthetic Clay Liner | 1.2 | 0 | 0 | 0 | 1.2 |

## Total Tensile Load

The total tensile load for each liner member is calculated by comparing the total strain calculated for the Trench 13 design to the strain at yield. For example:

(Yield strength of liner member (lbs/in))/(Total tensile load due to liner members (lbs/in)) = (Strain at yield of the liner member(%))/(Total Strain due to liner members (%)) where total tensile load due to liner members is the unknown.

Rearranging the equation:

Total tensile load due to liner members (lb/in) = Yield strength of liner member (lbs./in)/Strain at yield of liner member*Total strain due to liner members(%).

Example using the 60-Mil HDPE where:

Yield strength of liner member = 132 lbs/in
Strain at yield of liner member= 13%
Total strain due to liner members = 0.70%

Therefore, total tensile strength at load for the 60-Mil HDPE:

$$\frac{132 lbs/in}{13\%} * 0.70\% = 7.1 lbs/in$$

**Table 6: Total Tensile Load on Liner Members**

| Material | Yield Strength *(lb/in)* | Strain at Yield *%* | Total Strain *%* | Total Tensile Load *lbs/in* |
|---|---|---|---|---|
| Sacrificial 40 Mil HDPE Liner | 84 | 12 | 4.9 | 34 |
| 10oz Non-woven Geotextile | 150 | 50 | 4.3 | 13 |
| Geonet – LCRS Side Slope – 200 Mil | 45 | 23 | 5.3 | 10 |
| 80 Mil HDPE Single Sided Texture | 176 | 13 | 0.57 | 7.8 |
| LDS Side Slope Geocomposite 6 oz double-sided 200 Mil | 50 | 50 | 1.1 | 1.1 |
| 60 Mil HDPE Double Sided Texture | 132 | 13 | 0.69 | 7.0 |
| Geosynthetic Clay Liner | 50 | 15 | 1.2 | 4.0 |

To avoid failure of any of the liner members, the calculated total tensile load for each liner member in the Trench 13 design must not exceed the tensile strength at yield. Factors of safety must be applied to the strength at yield, resulting in an allowable tensile load for each liner member. The total allowable tensile load on each liner member is calculated by the following equation:

$T_{allow} = T_{ultimate}$/Factors of Safety

Where:

$T_{ultimate}$ = ultimate tensile strength = tensile strength at yield

**Geotextile**

The equation to calculate allowable tension for the geotextile member of the liner system (Koerner, 1998 – **Reference 2**) is as follows:

$$T_{allow} = T_{ultimate}\left(\frac{1}{RF_{ID} * RF_{CR} * RF_{CD} * RF_{BD}}\right)$$

Where

$T_{allow}$ = allowable tensile strength
$T_{ultimate}$ = ultimate tensile strength = tensile strength at yield

The maximum reducing factors for geotextiles used in a separation capacity are:

$RF_{ID}$ = reduction factor for installation damage = 2.5
$RF_{CR}$ = reduction factor for creep = 2.5
$RF_{CD}$ = reduction factor for chemical degradation = 1.5
$RF_{BD}$ = reduction factor for biological degradation = 1.2

Inserting these values into the equation yields:

$T_{allow} = T_{ultimate}$ /11.25
For geotextile, $T_{ultimate}$ = 150 pounds/inch
$T_{allow}$ = 150/11.25 = 13.3 pounds/inch
As calculated above, total tensile load – 13 lbs/in

Since $T_{allow}$ > total tensile load, the material is safe from failure.

**Geonet**

Factors of safety for tensile loading and strain of Geonets were unavailable, so a factor of safety of 4 was applied (factor of safety used for geonet evaluation in 1996 and 2007 Trench 12 Design).

$T_{allow} = T_{ultimate}/4.0$
For geonet, $T_{ultimate}$ = 45 pounds/inch, therefore
$T_{allow}$ = 45/4 = 11 pounds/inch
As calculated above, total tensile load = 10 lbs/in

Since $T_{allow}$ > total tensile load, the material is safe from failure

**HDPE**

Factors of safety for HDPE Geomembranes range from 10 to 100 times (Koerner **Reference 2**). A safety factor of 10 is used in this analysis.

**Sacrificial 40 Mil Liner**

For the sacrificial 40 Mil HDPE, $T_{ultimate}$ = 63 lbs/in, therefore
$T_{allow}$ = 84/10 = 8.4 lbs/in
As calculated above, total tensile load = 34 lbs/in

Since $T_{allow}$ < total tensile load, the material is subject to failure. In this case, the sacrificial liner is strictly for protection of the geotextile from the elements, specifically harmful UV rays. The 40 Mil liner is intended to deteriorate as waste in being placed in the Trench, the resulting calculation is considered irrelevant for the purposes of this design.

**80 Mil HDPE Liner**

For the upper 80 Mil HDPE, $T_{ultimate}$ = 176 lbs/in, therefore
$T_{allow}$ = 176/10 = 18 lbs/in
As calculated above, total tensile load = 7.7 lbs/in

Since $T_{allow}$ > total tensile load, the material is safe from failure.

**60 Mil HDPE Liner**

For the lower 60 Mil HDPE, $T_{ultimate}$ = 132 lbs/in, therefore
$T_{allow}$ = 132/10 = 13 lbs/in
As calculated above, total tensile load = 7.1 lbs/in

Since $T_{allow}$ > total tensile load, the material is safe from failure.

**Geocomposite**

No recommended reducing factors were available for geocomposites; therefore, a safety factor of 4 was used (factor of safety used for geocomposite evaluation in 1996 and 2007 Trench 12 Design). Inserting this reducing factor into the equation yields:

$T_{allow} = T_{ultimate} /4.0$

For geocomposite, $T_{ultimate}$ = 50 pounds/inch, therefore

$T_{allow}$ = 50/4 = 13 pounds/inch

As calculated above, total tensile load = 1.1 lbs/in

Since $T_{allow}$ > total tensile load, the material is safe from failure.

**GCL**

No recommended reducing factors were available for GCLs; therefore, a safety factor of 10 was used (factor of safety used for GCL evaluation in 1996 and 2007 Trench 12 Design). Inserting this safety factor into the equation yields:

$T_{allow} = T_{ultimate} /10$

For GCL, $T_{ultimate}$ = 50 pounds/inch, therefore

$T_{allow}$ = 50/10 = 5.0 pounds/inch

As calculated above, total tensile load = 4.0 lbs/in

Since $T_{allow}$ > total tensile load, the material is safe from failure.

**Table 7: Allowable Tensile Load on Liner Members**

| Material | Yield Strength $T_{ultimate}$ *(lb/in)* | Safety Factor *%* | Allowable Tensile Load *lbs/in* | Total Tensile Load *lbs/in* | Allowable > Total |
|---|---|---|---|---|---|
| Sacrificial 40 Mil HDPE Liner | 84 | 10 | 8.4 | 34 | No |
| 10oz Non-woven Geotextile | 150 | 11.25* | 13 | 13 | Yes |
| Geonet – LCRS Side Slope – 200 Mil | 45 | 4 | 11 | 10 | Yes |
| 80 Mil HDPE Single Sided Texture | 176 | 10 | 18 | 7.8 | Yes |
| LDS Side Slope Geocomposite 6 oz double-sided 200 Mil | 50 | 4 | 13 | 1.1 | Yes |
| 60 Mil HDPE Double Sided Texture | 132 | 10 | 13 | 7.0 | Yes |
| Geosynthetic Clay Liner | 50 | 10 | 5.0 | 4.0 | Yes |

Note:
*Calculated as a product of 4 reduction factors, but is used to calculate an allowable tensile load in a similar manner as a safety factor.

## CONCLUSIONS

Liner material stability on Trench 13 side slopes of 0.5:1.0 were evaluated for liner material strength and ability to remain intact and function under the loads that will be imposed by liner material weight (self-weight of liner members and loading from overlying liner members) and resisted by liner strength and friction.

The materials specifications for the Trench 13 Liner System were provided from manufactures, and were consistent with the materials approved for Trench 12 construction. Values that were not provided in specification sheets were interpreted from technical articles and research papers, specifically the values for shear strength and friction angles between liner components. All technical documents are referenced and attached to this calculation.

Four strains were considered on the liner members including strain due to 1) self-weight, 2) thermal expansion, 3) seismic deformation, and 4) settlement of waste fill. Strains on individual members were summed as a total strain of the liner system. The total strain was compared to the manufacturer's technical specification strains at yield. A reduction factor (conservative safety factor) was used with the manufacturer's data. None of the liner member's calculated strains exceed the strain at yield provided in technical specifications except the sacrificial 40 Mil HDPE liner that serves only to provide UV protection and failures are expected.

Material to be approved for construction of the Trench 13 Liner System must meet or exceed specifications illustrated in this calculation or be independently verified by the design engineer and/or their representative.

**Figure 1: Forces Acting on Trench 13 Liner System**

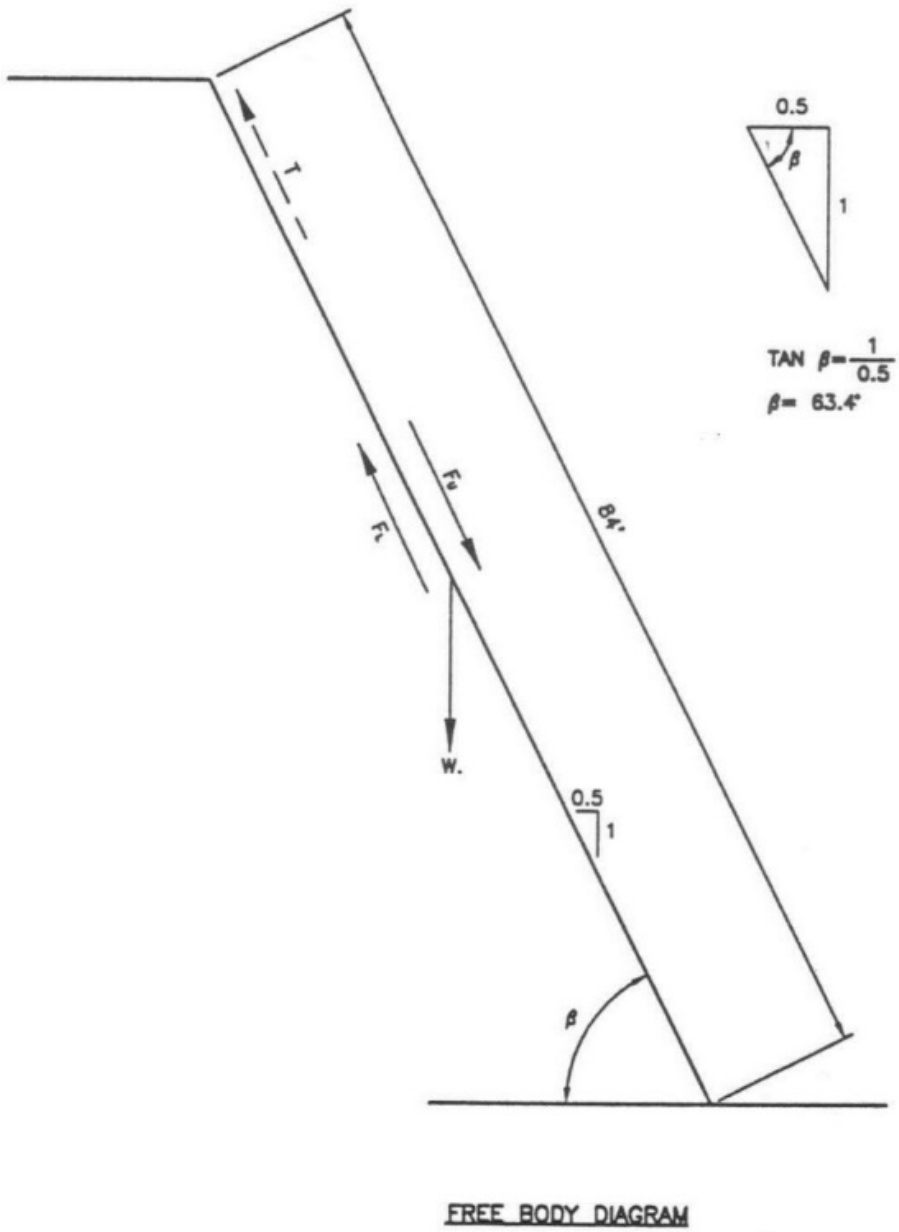

**Figure 2: Exploded View of Trench 13 Side Wall Liner System Components**

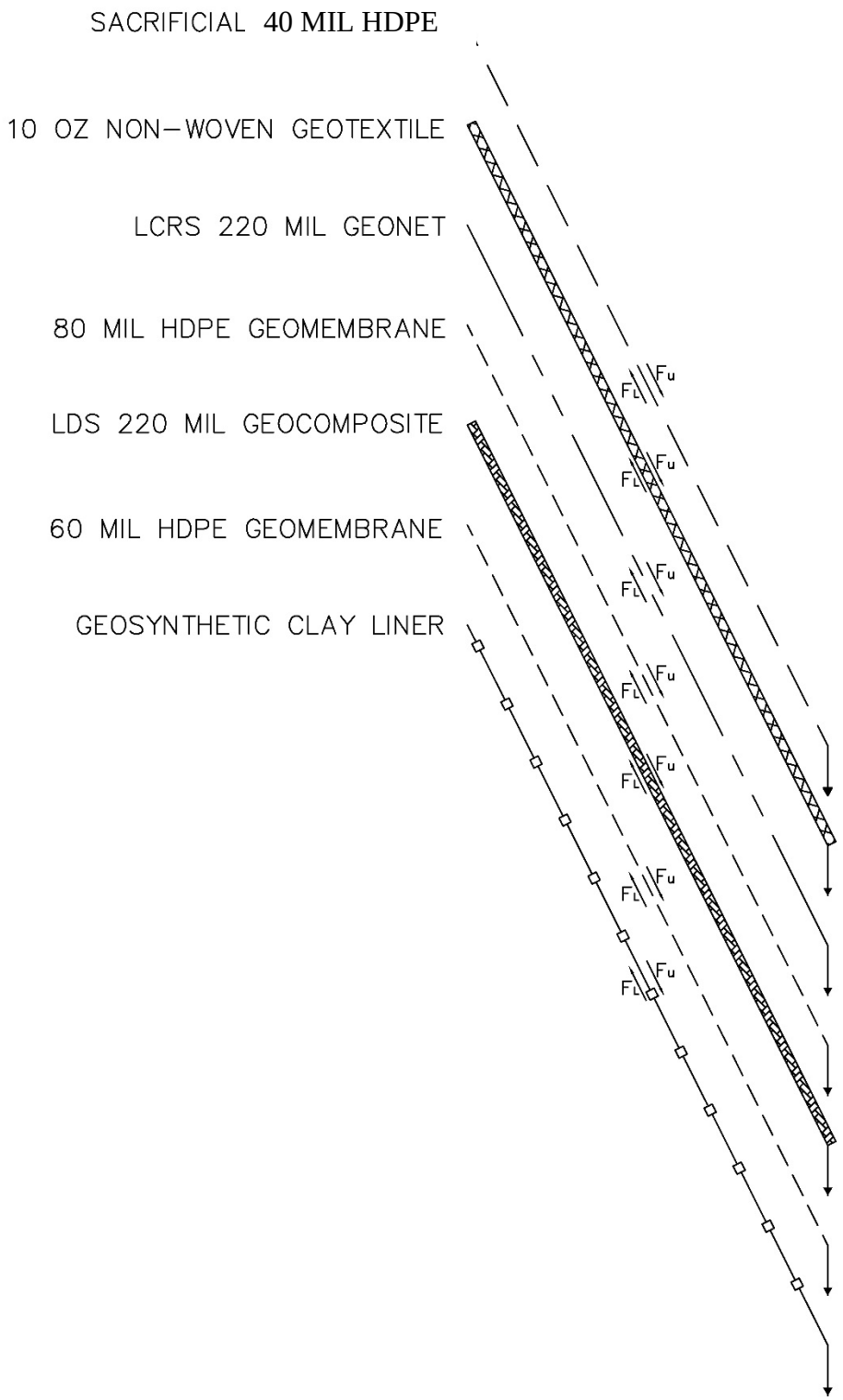

# REFERENCES

**Reference 1: Technical Journals for Interpretation of Friction Angles of Geosynthetics**

**Reference 1-A: Comparison of PVC and HDPE Geomembranes (Interface Friction Performance. K.Bhatia, Syracuse University**

**Reference 1-B: Estimation of Dynamic Interfacial Properties of Geosynthetics. De and Zimmie. 1998.**

**Reference 1-C: Interface Friction Test Results ASTM D 5321. Performed by Geotechnics, 2014**

**Reference 1-D: Interpretations of Cohesion and Friction Angles in Direct Shear Tests. Published by Cetco, Thiel, 2009.**

**Reference 1-E: Static Shear Strenght of Geosynthetic Clay Liners. Athanassopoulos and Fox. 2013.**

**Reference 2: Koerner, Robert 1994. Designing with Geosynthetics**

**Reference 3: Trench 12 Liner Material Properties – Used as basis for stability evaluation**

REFERENCE 1-A

A Report
on

# COMPARISON OF PVC and HDPE GEOMEMBRANES (INTERFACE FRICTION PERFORMANCE)

for

PVC GEOMEMBRANE INSTITUTE.

Dr.Shobha K.Bhatia
Gautam Kasturi
Dept. of Civil and Environmental Engineering
SYRACUSE UNIVERSITY

## 1.0 INTRODUCTION

Modem solid-waste landfills and hazardous landfills in the USA are required to have a low hydraulic conductivity liner and drainage system, consisting of geosynthetic materials (geomembranes, geotextiles, geonets and geocomposites) and compacted clay. A cross-section of a typical modem landfill, as shown in Figure 1.1, consists of several layers of soils and geosynthetic products. The stability of these 'slopes' is controlled by the shear strength of the various interfaces in such a composite liner. Critical interfaces include soil vs. geomembrane, soil vs. geotextile, geomembrane vs. geotextile and geomembrane vs. geonet. The strength of each of these interfaces has to be determined after careful, site-specific material testing (Koerner, 1994). The experience and confidence gained from these tests on different materials and soils is valuable to designers. Such data give the basis for better judgment in design. The importance of the evaluation of interface strength has been illustrated by the slope stability failure in Phase 1A of the construction of the Kettleman Landfill in California (Mitchell et al., 1990).

Geomembranes are critical components of modem landfill design, performing important functions moisture barriers in the containment system. Today, a variety of geomembranes are in use in current practice. The basic difference between them is the material and/or method of manufacture. The most commonly-used material types are (PVC) Poly Vinyl Chloride and (HDPE) High Density Poly-Ethylene. Based on a 1992 estimated total of 648 million sq. feet of geomembrane sales, HDPE accounts for 259 million sq. feet or 40 % of sales , while PVC accounts for 162 million sq. feet or 25 % of sales(Koerner, 1994). Very Low Density Poly-Ethylene (VLDPE), a Polyethylene product, which is more flexible than HDPE, accounts for 65 million sq. ft or 10 % of sales .

Geomembrane interface frictional failure has been identified as the cause of numerous geosynthetic-lined slope failures. As a result, the interface frictional strength of any geomembrane interface has to be determined with utmost care. It is recommended that wherever possible, the interface frictional strength for a geomembrane-soil combination be determined experimentally, without resorting to use of generalized values for similar soils from published data (Koerner, 1994). Direct shear, pullout and ring shear tests have been performed extensively, mainly on soil-geomembrane interfaces, to characterize their strengths (Koerner et al., 1986; Seed et al., 1988; O'Rourke et al., 1990; Takasumi et al, 1991; Stark and Poeppel, 1994)

There have been a limited number of testing programs that have attempted to draw a general comparison between HDPE and PVC geomembranes. O'Rourke (1990) reported that the higher the stiffness or hardness of the geomembrane, like HDPE, the lower the friction angle, as compared to a flexible membrane, like PVC. Martin et al. (1984) tested geotextile vs. geomembrane interface friction using a very soft, flexible geomembrane like Ethylene Propylene Diene Monomer (EPDM), a medium stiffness PVC geomembrane and a tough geomembrane like HDPE. They also concluded that the softer geomembranes, have greater friction angles than the tougher geomembranes.

**Table 2.1 Properties of Geomembranes used in the Testing Program**

| GEOMEMBRANE TYPE | *SMOOTH PVC[1]* | *TEXTURED PVC[2]* | *FILE-FINISH PVC[3]* | *SMOOTH HDPE[4]* | *TEXTURED HDPE[5]* |
|---|---|---|---|---|---|
| MANUFACTURER | Oxychem | **OxyChem** | **C.G.T. Ltd.** * | **GSE**** | **GSE** |
| TRADE NAME | **Oxyflex** | **OxyGrip** | **Taffeta** | **GSEHD** | **GSEHDT** |
| GAUGE ( mils ) | 30 | 30 | 30 | 60 | 60 |

* Canadian General Towers
** Gundle / SLT Environmental ( Inc. ) Company
1. Smooth PVC : Smooth, flexible PVC geomembrane
2. Textured PVC : PVC geomembrane, with extrusions of 4 - 6 mils on the surface, giving the rough texture. The textured surface was used as the interface
3. File-Finish PVC : Square grid etched onto one surface, with smooth PVC on the other surface. The surface with the file-finish was used as the interface.
4. Smooth HDPE : Smooth, tough, inflexible HDPE geomembrane
5. Textured HDPE : Co-extruded textured surface on one side and smooth HDPE on the other surface. The textured surface was used in the surface.

2.1.2 Soil

A typical landfill consists of soil-geomembrane interfaces involving a variety of soils. Most commonly, sand as a drainage layer and clay as a moisture barrier are used. However, when locally available soils are the only option, sandy loam and silty clay are used as substitutes. Hence, these soils were also included in this study. Figure 2.1 gives the grain size distribution of the soils.

*2.1.2.1 Sand*

Sand-Geomembrane interfaces are common at the boundary of a drainage layer and the next layer of moisture barrier. Testing for this interface was performed using sand with the following properties :

Grain size distribution :

$D_{10}$ - 0.15 mm $D_{50}$ - 0.29 mm $D_{90}$ - 0.51 mm
$C_u$ - 2.13 $C_c$ - 0.919
Internal Friction : Angle of Internal Friction, from a Direct Shear Test = 32.3"

This sand can be described as uniform, fine sand. It was mixed with just enough water to simulate the average field wetness conditions (approximately 10%).

### 2.1.2.2 *Sandy Loam*

In many situations, the soils most suitable for a landfill may not be available on location. In such cases, liners are constructed with the available soil. One of the common soils found at sites is sandy loam. In such situations, sandy loam is used as an alternative to sands in the landfill. The soil used for testing in this program can be described as well graded sandy loam. In this soil, there was a significant amount of organic matter, including plant root fibers and remains of insects. The natural water content of the soil was 41.8 % . Testing was done at the same water content.

The requirements of a material to be used as drainage material in a waste containment system are as follows ( USEPA, 1989 ) :

- Hydraulic conductivity must be greater than $10^{-2}$ cm / s ;
- Rounded to sub-rounded material, to avoid damage to the adjacent geosynthetics ;
- Well graded material ; and
- Maximum particle size of 3 / 8 inch ( 9.5 mm ) .

The properties of the sandy loam used in this study were :

<u>Grain size distribution characteristics</u> :

| | | |
|---|---|---|
| $D_{10}$ - 0.10 mm | $D_{50}$ - 0.53 mm | $D_{90}$ - 4.2 mm |
| $C_u$ - 9.0 | $C_c$ - 0.69 | |

Based on the USEPA requirements above for a drainage material, the sandy loam tested satisfies the requirements for use as a drainage material. The hydraulic conductivity requirement needs to be verified, but it is strongly believed that it will be complied, based on its grain size distribution.

### 2.1.2.3 *Silty Clay*

Locally available soil is generally preferred for the compacted clay layer in a landfill liner. In such cases, the criteria for selecting the soil are(Daniel, 1993) :

- % dry weight passing the #200 sieve >= 39 % - 50 %
- % dry weight retained on the # 4 sieve <= 20 % - 50 %
- PI (ASTM D 4318) >= 7 % - 10%
- Maximum grain size : 25 mm - 50 mm

<u>Grain size distribution characteristics</u> :

| | | |
|---|---|---|
| $D_{10}$ - < 0.075 mm | $D_{50}$ - 0.12 mm | $D_{90}$ - 4.3 mm |
| $C_u$ - 23.17 | $C_c$ - 1.03 | |

Similarly, the stress measured was that between the geomembrane and the soil as well, because those were the only two materials in contact as the top box moved relative to the bottom box.

The high value of $R^2$ for the graph of the failure envelope ( Figure 3.2(b) ) indicates that the $\phi$ value for this interface was not affected by the confining stress level, although it may be different for much lower confining stresses ( less than 10 kPa ).

### 3.2 Sand vs. the Other Geomembranes

The relationships for fine sand vs. smooth HDPE interface are shown in Figures 3.3 (a) and (b). The same relationships, stress vs. displacement and interface friction angle, for sand vs. the rest of the geomembranes in the testing program, are given in Appendix A. Stretching was observed in the File-finish PVC interface at higher normal stresses (greater than 100 kPa). Strain softening behaviour was noticed with HDPE. Textured HDPE exhibited peak values at higher displacements (about 35 mm). However, textured PVC did not reveal a clear trend in its stretching.

### 3.3 Influence of Soil Type

The study of the variation of interface friction values of the same geomembranes with soil type shows considerable difference in the stress-strain behaviour as well as friction angle values. Figures 3.4 and 3.5 give relationships of smooth PVC interfaces against sandy loam and silty clay respectively. Figures showing these relationships for interfaces with other geomembranes are given in Appendix B (Sandy Loam) and Appendix D (Silty Clay).

### 3.4 Geomembrane vs. Geotextile

The relationships for the smooth PVC vs. geotextile interface are shown in Figure 3.6. Interface friction values of the other geotextile-geomembrane interfaces are given in Appendix D.

## 4.0 SUMMARY OF RESULTS

The results of the testing program are summarized in Tables 4.1 and 4.2. The interface friction angles based on stress obtained at about 10 % strain (25.4 mm) from the stress displacement curves are given in Table 4.1. Table 4.2 gives the interface friction angles based on the peak stress obtained from the stress-displacement graphs. In the case of HDPE and textured-HDPE membranes, the stress-displacement response of the interface is such that after reaching peak stress, further shearing to a larger strain causes stabilization of the stress (remains constant ; see Figure 3.3). Hence, the shear stress at 10% strain for the rigid membranes (HDPE and HDT) is less than at the peak. However, for the flexible membranes (PVCs), due to their stretching during the tests, the strength at higher strain is greater than at lower strain (see Figure 3.4). This was observed with all PVC interfaces with all the other interface materials except with fine sand.

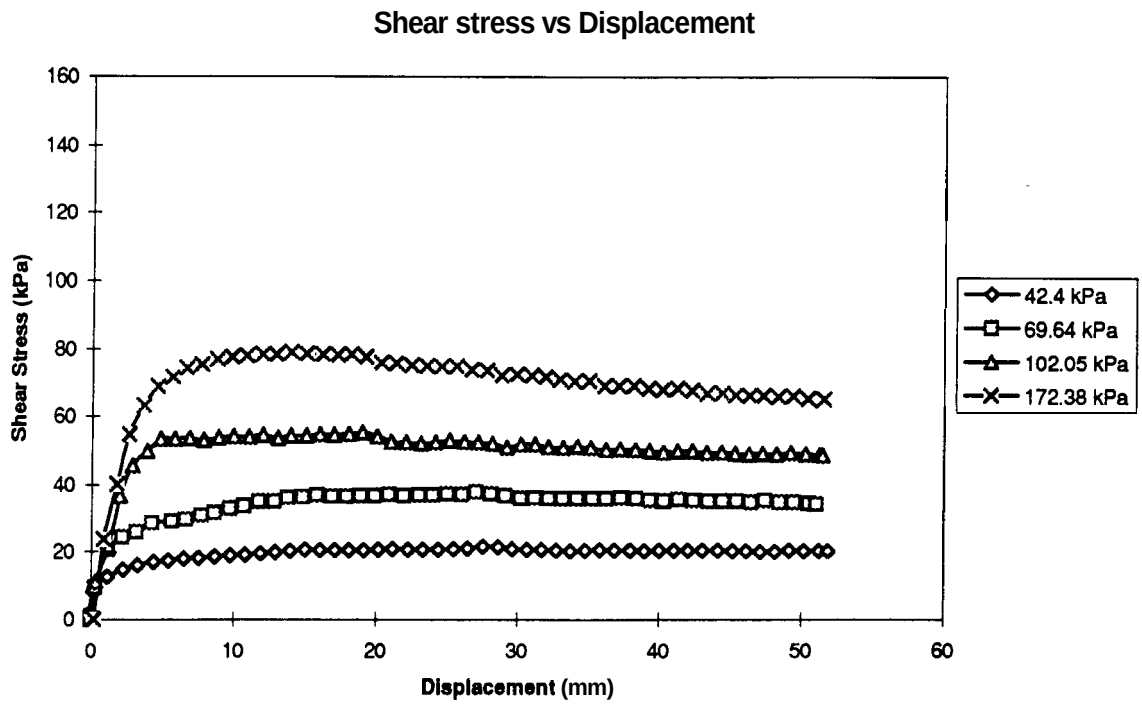


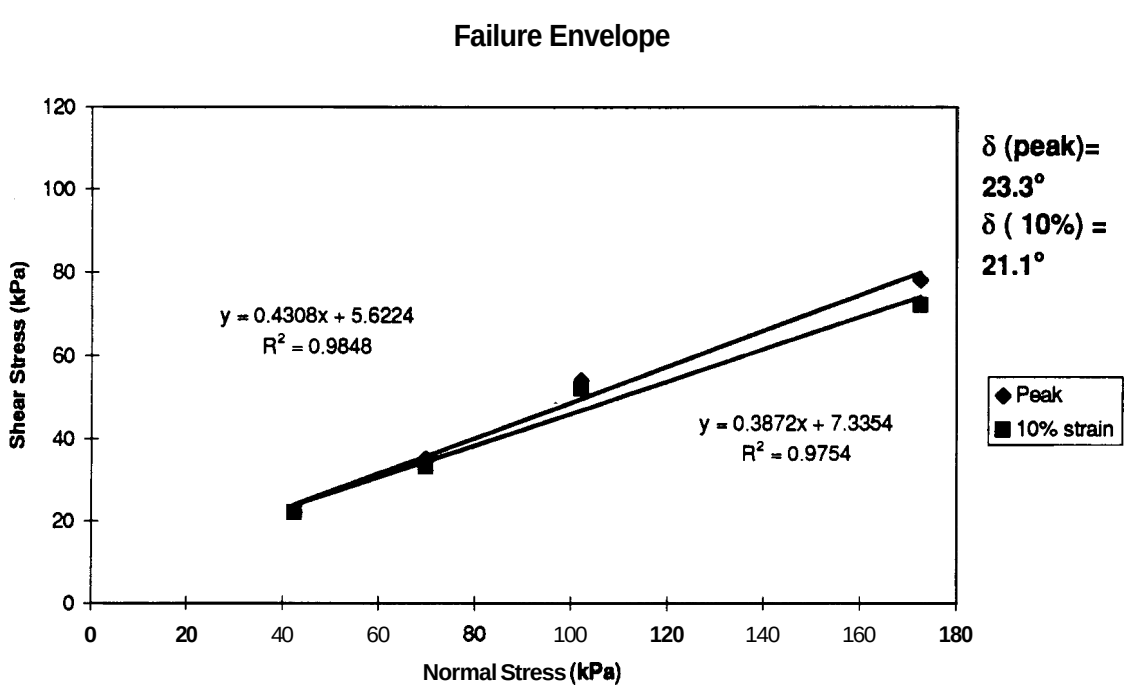


Figure 3.3 Fine Sand vs Smooth HDPE a) Shear vs Displacement b) Friction Angle

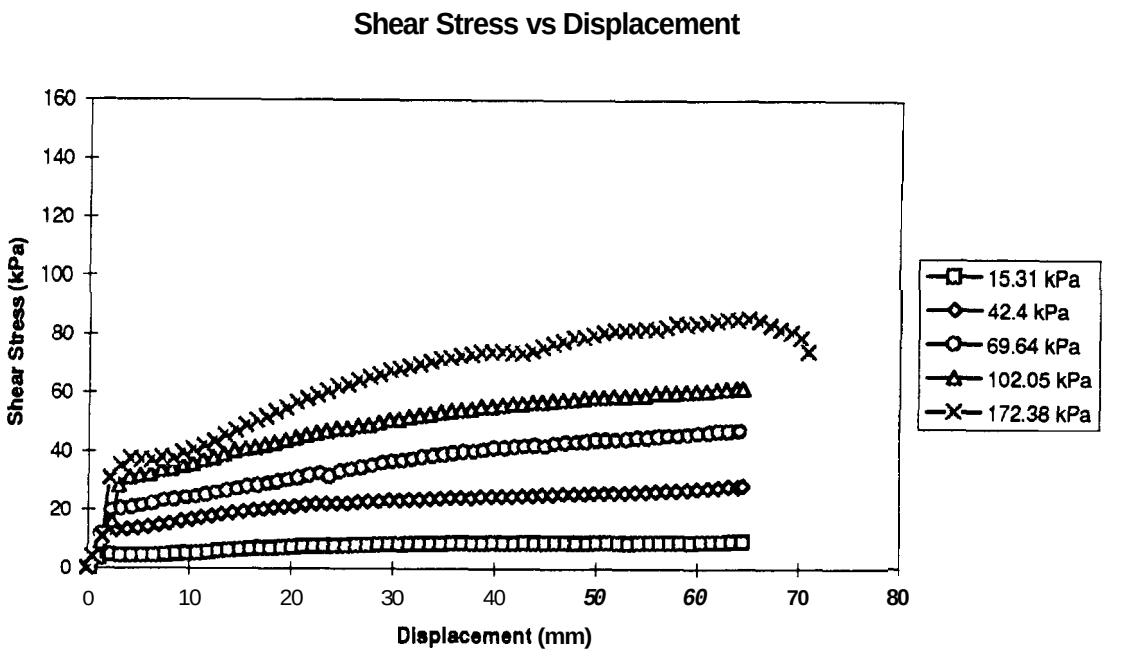


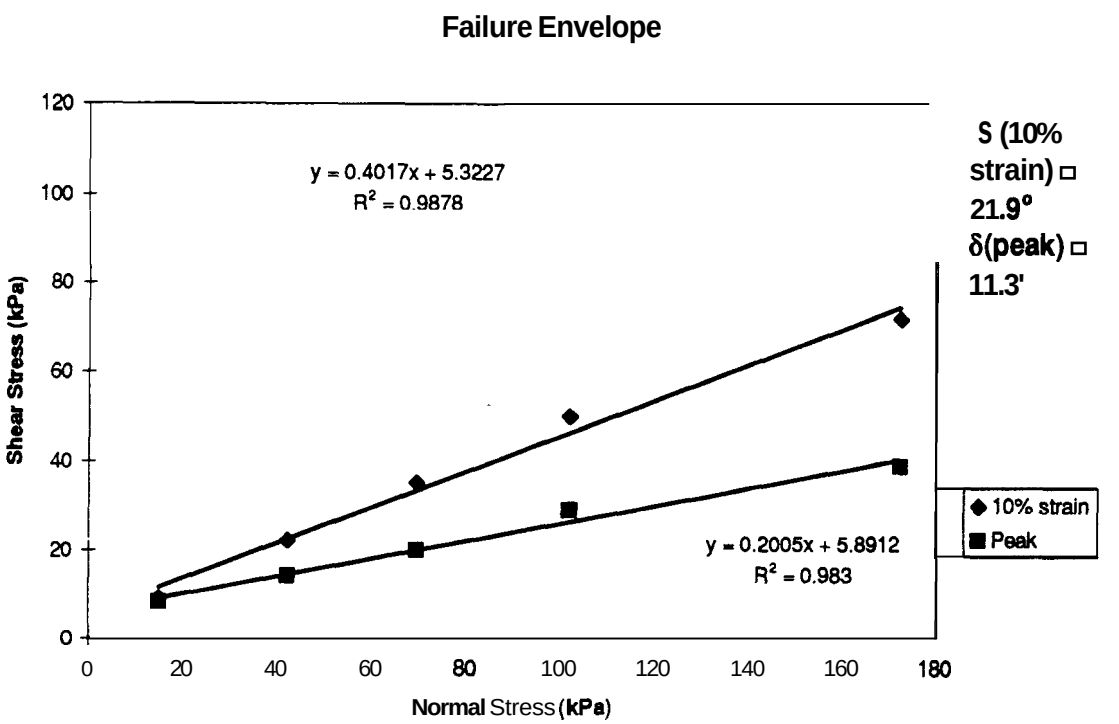


Figure 3.6 Non-Wovemn Geotextile vs. Smooth PVC a)Stress vs. Displacement b) Friction Angle

For this reason, the friction angle for the interfaces were calculated at both the peak stress and the stress at 10 % strain. It can be readily seen, comparing Tables 4.1 and 4.2, that the interface angle for PVC membranes at initial peak (yield stress for the interface) is much lower than at higher strain. However, the yield point of the interface does not represent a failure condition. This is because further shearing causes an increase in strength and not a decrease, whereas further shearing in HDPE causes reduced strength. Therefore, under field conditions, if the PVC membranes are stressed beyond the yield stress for the interface, the material stretches under the load without any loss of strength or material damage.

**Table 4.1 Interface Friction Angle values ( degree )obtained for various interfaces tested ( at 10 % strain )**

| | Fine Sand | Sandy Loam | Silty Clay | Non-woven Geotextile |
|---|---|---|---|---|
| 30 mil Smooth PVC ( at 10 % strain ) | 34.7 | 26.4 | 20.8 | 21.9 |
| 30 mil textured PVC ( at 10 % strain ) | 35.3 | 21.1 | 26.4 | 19.6 |
| 30 mil File-finish PVC ( at 10 % strain ) | 30.9 | 28.1 | 26.0 | 17.3 |
| 60 mil Smooth HDPE ( at 10 % strain ) | 21.1 | 18.2 | 17.0 | 14.2 |
| 60 mil Textured HDPE ( at 10 % strain ) | 36.6 | 33.8 | 41.8 | 17.4 |

**Table 4.2 Interface Friction Angle values ( degree )obtained for various interfaces tested ( at Peak Stress )**

| | Fine Sand | Sandy Loam | Silty Clay | Non-woven Geotextile |
|---|---|---|---|---|
| 30 mil Smooth PVC ( Peak stress ) | 34.7 | 26.4 | 21.5 | 11.3 |
| 30 mil textured PVC ( Peak stress ) | 35.3 | 19.9 | 22.9 | 13.2 |
| 30 mil File-finish PVC ( Peak stress ) | 30.9 | 28.1 | 27.7 | 11.4 |
| 60 mil Smooth HDPE (Peak stress ) | 23.6 | 25.2 | 25.8 | 15.1 |
| 60 mil Textured HDPE ( Peak stress ) | 36.6 | 33.8 | 41.8 | 17.4 |

REFERENCE 1-B

## Technical Paper by A. De and T.F. Zimmie

# ESTIMATION OF DYNAMIC INTERFACIAL PROPERTIES OF GEOSYNTHETICS

**ABSTRACT:** The dynamic frictional properties of different geosynthetic interfaces play an important role in the stability analyses of various geotechnical structures that incorporate geosynthetics. The paper presents and discusses laboratory test results on eight different interfaces, formed through various combinations of three geosynthetics (a geotextile, a smooth geomembrane, and a geonet). The dynamic frictional properties were estimated using cyclic direct shear tests, shaking table tests conducted at a normal g-level of 1g as well as at high g-levels, and on a 100 g-ton geotechnical centrifuge. The centrifuge simulated high normal stress levels, commonly encountered by geosynthetics comprising base liners of landfills or base isolators for large structures. The tests revealed various important characteristics regarding the dynamic frictional properties of the geosynthetic interfaces, including a dependence of some of the interfaces on the level of normal stress and the excitation frequency. It is felt that these differences should be considered when selecting proper test methods in relation to the application for which the geosynthetic is considered. It was concluded that proper simulation of field conditions in laboratory experiments is important to obtain suitable friction angle values to be used in design.

**KEYWORDS:** Landfill liner, Geotextile, Geomembrane, Geonet, Dynamic friction angle, Cyclic shear test, Shaking table, Geotechnical centrifuge.

**AUTHORS:** A. De, Senior Staff Engineer, GeoSyntec Consultants, 1500 Newell Avenue, Suite 800, Walnut Creek, California 94596, USA, Telephone: 1/925-943-3034, Telefax: 1/925-943-2366, E-mail: anirbande@geosyntec.com; and T.F. Zimmie, Professor, Department of Civil Engineering, Rensselaer Polytechnic Institute, Troy, New York 12180, USA, Telephone: 1/518-276-6939, Telefax: 1/518-276-4833, E-mail: zimmit@rpi.edu.

**PUBLICATION:** *Geosynthetics International* is published by the Industrial Fabrics Association International, 1801 County Road B West, Roseville, Minnesota 55113-4061, USA, Telephone: 1/612-222-2508, Telefax: 1/612-631-9334. *Geosynthetics International* is registered under ISSN 1072-6349.

**DATES:** Original manuscript received 30 July 1997, revised version received 17 December 1997 and accepted 2 January 1998. Discussion open until 1 September 1998.

**REFERENCE:** De, A. and Zimmie, T.F., 1998, "Estimation of Dynamic Interfacial Properties of Geosynthetics", *Geosynthetics International*, Vol. 5, Nos. 1-2, pp. 17-39.

## 1 INTRODUCTION

The frictional properties of different geosynthetic interfaces play an important role in the stability analyses of various geotechnical structures that incorporate geosynthetics. Many of the geosynthetic surfaces in composite liner systems of modern landfills are characterized by relatively low friction angles. This causes the interfaces between such elements to be likely locations for slip movement. Recent requirements to include considerations for seismic impact in modern landfill designs have led to the need for understanding the dynamic frictional properties of these interfaces. The use of different types of geosynthetic materials for the purpose of base isolation also requires estimation of the dynamic frictional properties of the interfaces under suitable loading conditions and frequencies of excitation.

## 2 BACKGROUND

The importance of interfacial frictional properties of geosynthetics in landfill design was demonstrated by the Kettleman Hills, California landfill failure which occurred in 1988. Subsequent analyses led to extensive research into the static or monotonic frictional properties of geosynthetic interfaces (Mitchell et al. 1990a; Mitchell et al. 1990b; Byrne et al. 1992; Stark and Poeppel 1994). The most common apparatuses/methods used to estimate the static friction angles included direct shear devices (both small- and large-size), pull-out boxes, and ring shear devices. Some of the results from these studies demonstrated unique trends that were characteristic of the different testing procedures.

As a result of this extensive range of testing programs, a broad understanding of the characteristic features of different static (or monotonic) testing methods is available. Gilbert et al. (1995) have compiled a summary of the advantages and disadvantages associated with different test devices that measure interface shear strength. The devices included in the summary are the large-scale direct shear box, conventional direct shear box, torsional shear device, tilt table, and Texas double shear device.

### 2.1 Dynamic Friction Tests

Experimental research to estimate the dynamic frictional properties of geosynthetic/geosynthetic interfaces has been conducted relatively recently (Hushmand and Martin 1990; Kavazanjian et al. 1991; Yegian and Lahlaf 1992b; Pasqualini et al. 1995; Zimmie et al. 1994; Yegian and Harb 1995; De 1996). The following apparatuses were used in these studies:

- a cyclic direct shear device (Pasqualini et al. 1995; De 1996);
- a shaking table device (Yegian and Lahlaf 1992b; Hushmand and Martin 1990; Zimmie et al. 1994; De 1996); and
- a shaking table device on a geotechnical centrifuge (Hushmand and Martin 1990; Zimmie et al. 1994; De 1996).

**Table 1. Description of the geosynthetic interfaces.**

| Interface number | Geosynthetic A | Geosynthetic B |
|---|---|---|
| I | Geotextile | Smooth geomembrane |
| II | Smooth geomembrane | Geonet (transverse) |
| III | Smooth geomembrane | Geonet (longitudinal) |
| IV | Smooth geomembrane | Geonet (aligned) |
| V | Geotextile | Geonet (transverse) |
| VI | Geotextile | Geonet (longitudinal) |
| VII | Geotextile | Geonet (aligned) |
| VIII | Smooth geomembrane | Smooth geomembrane |

### 3.2.1 *Cyclic Direct Shear Device*

The direct shear apparatus used in the current study was fabricated for testing geosynthetic specimens 300 mm × 300 mm in dimension. The shear force was applied through a hydraulic actuator controlled by an MTS™ control unit. The normal force was applied by means of a pneumatic piston and compressed air. Fixed amplitudes of displacement were produced on both sides of the mean specimen position. Measurements of shear force and displacement were made continuously by means of load cells and a linear variable differential transformer (LVDT).

### 3.2.2 *Shaking Table Apparatus*

An electro-hydraulic shaking table that can accommodate specimens with dimensions up to 560 mm × 380 mm was used for the shaking table tests. Sinusoidal base motion was produced through the use of a dynamic signal analyzer. The acceleration was measured during the experiments by means of accelerometers attached to the table and to the block, and the relative displacement between the block and the table was measured using two LVDTs. Data acquisition was performed using a personal computer with commercially available software.

### 3.2.3 *Geotechnical Centrifuge*

A 100 g-ton geotechnical centrifuge was used in which high normal stresses were produced to model prototype stress conditions. The shaking table apparatus was mounted on the centrifuge platform and experiments were performed at 10g, 20g, 30g, and 40g.

## 4.3 Geotextile Over a Geonet (Interfaces V, VI, and VII)

### 4.3.1 *Cyclic Direct Shear Tests*

Figure 9 shows the plots of peak dynamic friction angle versus number of cycles for the geotextile/geonet (transverse) interface (Interface V). The dynamic friction angle of this interface appears to be strongly dependent on the normal stress. The greatest friction angle value (approximately 24°) was obtained from tests at the lowest normal stress (20.7 kPa) and the lowest friction angle (approximately 17°) corresponded to the highest normal stress (41.4 kPa). In addition, for each test, there was little variation in the friction angle with the number of loading cycles.

A likely factor for the decrease in the friction angle with the increase of normal stress may be the highly deformable nature of nonwoven geotextiles when subjected to high normal stresses. The same interface showed a nonlinear shear versus normal stress behavior during monotonic testing (De 1996), and the same trend of higher normal stresses corresponding to the lower friction angle values was observed.

Results of the cyclic tests performed on Interfaces VI and VII showed friction angles to be relatively constant with the number of loading cycles, and the dynamic friction angle did not show a strong dependence on the normal stress. In each case, the dynamic friction angle values (15° for the longitudinal orientation, and between 10 and 11° for the aligned orientation) were close to those obtained from monotonic experiments reported elsewhere (De 1996).

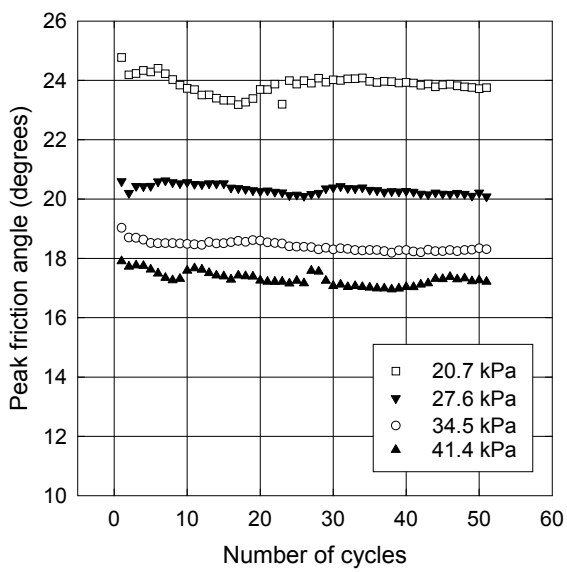


**Figure 9. Variation of the peak friction angle with the number of cycles from cyclic direct shear tests: a geotextile over a geonet (transverse) (Interface V).**

### 4.3.2 *Shaking Table Tests*

Shaking table tests on geotextile/geonet interfaces were performed using two orientations of the geonet: transverse and longitudinal. Figure 10 shows the test results for the geotextile/geonet (transverse) interface. The break point (i.e. the point at which the acceleration of the block fails to increase at the same rate as the acceleration of the table) occurs at an acceleration of 0.44g, corresponding to a dynamic friction angle of 24°. The geotextile/geonet (longitudinal) test results were similar and indicated an acceleration of 0.34g at the break point, and a dynamic friction angle of 19°.

### 4.3.3 *Shaking Table Tests Using a Geotechnical Centrifuge*

The results from the experiments performed at different acceleration levels for Interfaces V and VI are shown in Tables 5 and 6, respectively. From Table 5 it can be seen that the dynamic friction angles for Interface V at 1g, 30g, and 40g are 24°, 8°, and 7°, respectively. This shows a significant dependence on the normal stress; similar to what was observed for the cyclic direct shear test results on the same interface (Figure 9). In the case of Interface VI, the friction angle varies from 19° at 1g to approximately 10° at 40g. Centrifuge shaking table experiments were not conducted on a geotextile/geonet (aligned) interface (Interface IV).

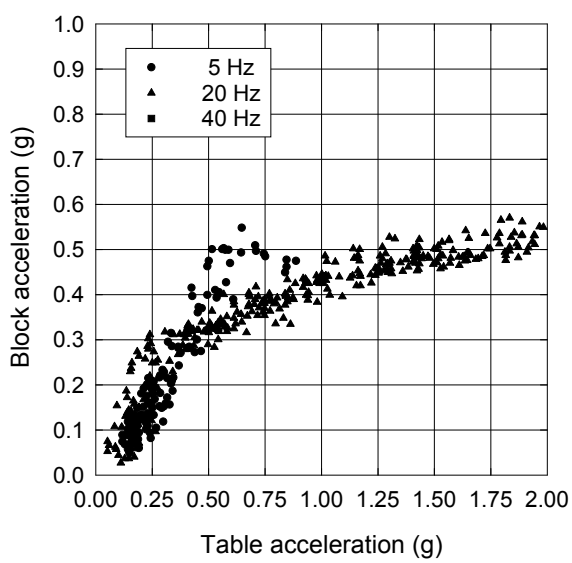


**Figure 10. Block versus table accelerations from shaking table tests: a geotextile over a geonet (transverse) (Interface V).**

**Table 5. Results from centrifuge shaking table experiments using a geotextile over a geonet (transverse) (Interface V).**

| g-level (g) | Shaking table acceleration at the inception of sliding (g) | Coefficient of dynamic friction ( = Column 2 ÷ Column 1) | Dynamic friction angle |
|---|---|---|---|
| 1 | 0.45 | 0.44 | 24° |
| 30 | 4.00 | 0.13 | 8° |
| 40 | 5.00 | **0.13** | 7° |

**Table 6. Results from centrifuge shaking table experiments using a geotextile over a geonet (longitudinal) (Interface VI).**

| g-level (g) | Shaking table acceleration at the inception of sliding (g) | Coefficient of dynamic friction ( = Column 2 ÷ Column 1) | Dynamic friction angle |
|---|---|---|---|
| 1 | 0.34 | 0.34 | 19° |
| 20 | 4.00 | 0.20 | 11° |
| 30 | 6.00 | 0.20 | 11° |
| 40 | 7.00 | 0.18 | 10° |

#### 4.3.4 *Results*

From the results shown in Section 4.3, it can be concluded that the behavior of the geotextile/geonet interfaces appears to show a dependence on the normal stress. This dependence is strong in the case of a transversely-orientated geonet (Interface V) and not as pronounced in the case of a longitudinally-orientated geonet (Interface VI).

### 4.4 Smooth Geomembrane Over a Smooth Geomembrane (Interface VIII)

#### 4.4.1 *Cyclic Direct Shear Tests*

The results of cyclic direct shear tests on Interface VIII (geomembrane/geomembrane interface) are plotted in Figure 11. The peak dynamic friction angle shows a strong tendency to increase with the number of cycles in the first 20 cycles. Following that, the rate of increase reduces, even though the increase continues to the end of the experiment which occurred after 50 cycles. There is no evidence of dependence on normal stress for these test results.

The cause for the increase in the dynamic friction angle with an increasing number of cycles is not completely understood. However, at the end of the tests, visual inspection of the specimens clearly showed surface abrasion of the geomembrane along the direction of shear displacement. It is not clear whether such abrasion was caused by the rapid movement of one layer of HDPE against another, or by a foreign object, such as dust particles present at the interface. Regardless of the cause, it is obvious that the abrasions resulted in an increase in the dynamic friction angle during cyclic loading.

REFERENCE 1-B



## 5 SUMMARY AND CONCLUSIONS

### 5.1 Summary of Results

The dynamic frictional behavior of eight geosynthetic interfaces have been presented in the current paper. The dynamic friction angles of the interfaces have been estimated on the basis of cyclic direct shear experiments and shaking table tests, both at 1g and high g-levels. The values of the friction angle obtained from the different experiments are listed in Table 8. For comparison, the static friction angles from tilt table and direct shear tests presented by De (1996) are also shown in Table 8.

In general, the results shown in Table 8 indicate that the initial values of static and dynamic friction angles for the geosynthetic interfaces tested are similar. However, the dynamic behavior of most interfaces is complicated by a dependence on the frequency of excitation and the number of loading cycles.

It was observed that the dynamic shear strength of geotextile/smooth geomembrane interfaces decreases slightly when subjected to repeated cycles of shear loading. This is due to the polishing effect of the geotextile on the geomembrane.

**Table 8. Average values of the peak friction angle for different geosynthetic interfaces.**

| Interface description | Static friction angle | | Dynamic friction angle | | |
|---|---|---|---|---|---|
| | Tilt table tests | Direct shear tests | Direct shear tests | Shaking table tests | |
| | | | | 1g | 10g to 40g |
| Nonwoven geotextile over smooth geomembrane | 11.8° | 12° | Decreases from 12.5 to 10.5° | 12° | 11° |
| Smooth geomembrane over geonet (transverse) | 10.1° | 11.3° | Increases from 11 to 18° (for low $\sigma$) or 14° (for high $\sigma$) | 12° | 7° |
| Smooth geomembrane over geonet (longitudinal) | 9.8° | 11.3° | Increases from 10 to 18° (for low $\sigma$) or 16.5° (for high $\sigma$) | 12° | 11° |
| Smooth geomembrane over geonet (aligned) | 8.1° | 8.1° | Increases from 9 to 18° (for both low and high $\sigma$) | --- | --- |
| Nonwoven geotextile over geonet (transverse) | 24.5° | Ranges from 22° (at low $\sigma$) to 14.5° (at high $\sigma$) | Ranges from 24° (at low $\sigma$) to 17° (at high $\sigma$) | 24° | 8° |
| Nonwoven geotextile over geonet (longitudinal) | 13.9° | Ranges from 17° (at low $\sigma$) to 14° (at high $\sigma$) | 15° | 19° | 11° |
| Nonwoven geotextile over geonet (aligned) | 11.2° | 10.5 | 11 to 10° | --- | --- |
| Smooth geomembrane over smooth geomembrane | 13.1° | 8.8° | Increases from 10.3 to 19.5° | 19° | 13° |

REFERENCE 1-B



cerning test methods, depending on the intended functions of the interface being designed. The results of centrifuge shaking table tests on some of the interfaces indicate a dependence on normal stress and frequency. Therefore, the use of this approach should be supplemented by cyclic direct shear tests and 1g shaking table tests. Table 9 has been prepared to provide guidance to the design engineer in selecting the proper testing procedures and values for the estimation of dynamic friction angles.

## REFERENCES

Byrne, R.J., Kendall, J. and Brown, S., 1992, "Cause and Mechanism of Failure, Kettleman Hills Landfill B-19, Unit IA", *Stability and Performance of Slopes and Embankments-II*, Seed, R.B. and Boulanger, R.W., Editors, Geotechnical Special Publication No. 31, ASCE, Vol. 2, proceedings of a specialty conference held in Berkeley, California, USA, June 1992, pp. 1188-1215.

De, A., 1996, "*Study of Interfacial Friction of Landfill Geosynthetics: Static and Dynamic*", Ph.D. Thesis, Rensselaer Polytechnic Institute, Troy, New York, USA, 245 p.

Geotek, 1987, "*Direct Shear Testing of Friction Liner Material*", Report for Gundle Lining Systems, Project 21266, March 1987, 10 p.

Gilbert, R.B., Liu, C.N., Wright, S.G. and Trautwein, S.J., 1995, "A Double Shear Test Method for Measuring Interface Strength", *Proceedings of Geosynthetics '95*, IFAI, Vol. 3, Nashville, Tennessee, USA, February 1995, pp. 1017-1029.

Hushmand, B. and Martin, G.R., 1990, "*Final Report SBIR Phase I Study, Layered Soil-Synthetic Liner Base Isolation System*", Report submitted to the National Science Foundation Small Business Innovative Research Program, The Earth Technology Corporation, Long Beach, California, USA, 86 p.

Kavazanjian, E., Hushmand, B. and Martin, G.R., 1991, "Frictional Base Isolation Using a Layered Soil-Synthetic Liner System", *Proceedings of the Third U.S. Conference on Lifeline Earthquake Engineering*, Cassaro, M.A., Editor, ASCE Technical Council on Lifeline Earthquake Engineering Monograph No. 4, Los Angeles, California, USA, August 1991, pp. 1140-1151.

Ko, H-Y., 1988, "Summary of the state-of-the-art in Centrifuge Model Testing", *Centrifuges in Soil Mechanics*, Craig, W.H., James, R.G. and Schofield, A.N., Editors, Balkema, pp. 11-18.

Mitchell, J.K., Seed, R.B. and Seed. H.B., 1990a, "Kettleman Hills Waste Landfill Slope Failure. I: Liner-System Properties," *Journal of Geotechnical Engineering*, Vol. 116, No. 4. pp. 647-668.

Mitchell, J.K., Seed, R.B. and Seed H.B., 1990b, "Stability Considerations in the Design and Construction of Lined Waste Depositories", *Geotechnics of Waste Fills - Theory and Practice*, ASTM Special Technical Publication 1070, Landva, A. and Knowles, G.D., Editors, proceedings of a symposium held in Pittsburgh, Pennsylvania, USA, September 1989, pp. 209-224.

Pasqualini, E., Sani, D. and Roccato, M., 1995, "Factors Influencing Geomembrane Interface Friction", *Green '93*, Sarsby, R.W., Editor, Balkema, proceedings of a conference held in Bolton, United Kingdom, June 1993, pp. 349-356.

REFERENCE 1-B



Schofield, A.N., 1980, "Twentieth Rankine Lecture: Cambridge Geotechnical Centrifuge Operations", *Geotechnique*, Vol. 20, No. 3, pp. 227-268.

Stark, T.D. and Poeppel, A.R., 1994, "Landfill Liner Interface Strengths from Torsional-Ring-Shear Tests", *Journal of Geotechnical Engineering*, Vol. 120, No. 3, pp. 597-615.

Von Pein, R.T. and Lewis, S.P., 1991, "Composite Lining System Design Issues", *Geotextiles and Geomembranes*, Vol. 10, Nos. 5-6, pp. 125-131.

Yegian, M.K. and Harb, J.N., 1995, "Slip Displacements of Geosynthetic Systems Under Dynamic Excitation", *Earthquake Design and Performance of Solid Waste Landfills*, Yegian, M.K. and Finn, W.D.L., Editors, Geotechnical Special Publication No. 54, ASCE, proceedings of a specialty conference held in San Diego, California, USA, October 1995, pp. 212-236.

Yegian, M.K. and Lahlaf, A.M., 1992a, "Discussion of 'Kettleman Hills Waste Landfill Slope Failure. I: Liner-System Properties' by Mitchell, J.K., Seed, R.B. and Seed. H.B.", *Journal of Geotechnical Engineering*, Vol. 118, No. 4, pp. 643-645.

Yegian, M.K. and Lahlaf, A.M., 1992b, "Dynamic Interface Shear Strength Properties of Geomembranes and Geotextiles", *Journal of Geotechnical Engineering*, Vol. 118, No. 5, pp. 760-778.

Zimmie, T.F., De, A. and Mahmud, M.B., 1994, "Centrifuge Modelling to Study Dynamic Friction at Geosynthetic Interfaces", *Proceedings of the Fifth International Conference on Geotextiles, Geomembranes and Related Products*, Vol. 1, Singapore, September 1994, pp. 415-418.

REFERENCE 1-C

# INTERFACE FRICTION TEST RESULTS

## ASTM D 5321

geotechnics
INTEGRITY IN TESTING

CLIENT : King Construction Services, Inc.
CLIENT PROJECT : Horry County East Hill Closure
PROJECT NO. : L14061-01
LAB I. D. NO.: Skaps TN 300-2-6 Geocomposite (L14061-01-02)
Agru 40 mil LLDPE Microspike, Roll # 343519-11 (L14061-01-01)

INTERFACE : **Geocomposite**
**vs. 40 mil LLDPE Microspike (Bottom/Shiny Side)**

| | PEAK SHEAR | RESIDUAL SHEAR |
|---|---|---|
| FRICTION ANGLE (deg) : | Φ = 32.1 | Φ = 15.0 |
| COEFFICIENT OF FRICTION : | = 0.628 | = 0.269 |
| ADHESION [Calculated] (psf): | a = 19 | a = 42 |

NOTES:
1.) The interface was loaded, inundated with water and seated for 1 hour prior to shearing.
2.) The peak friction angle was calculated using linear regression on the three data points.
3.) The residual friction angle was calculated using linear regression on the end of test values.

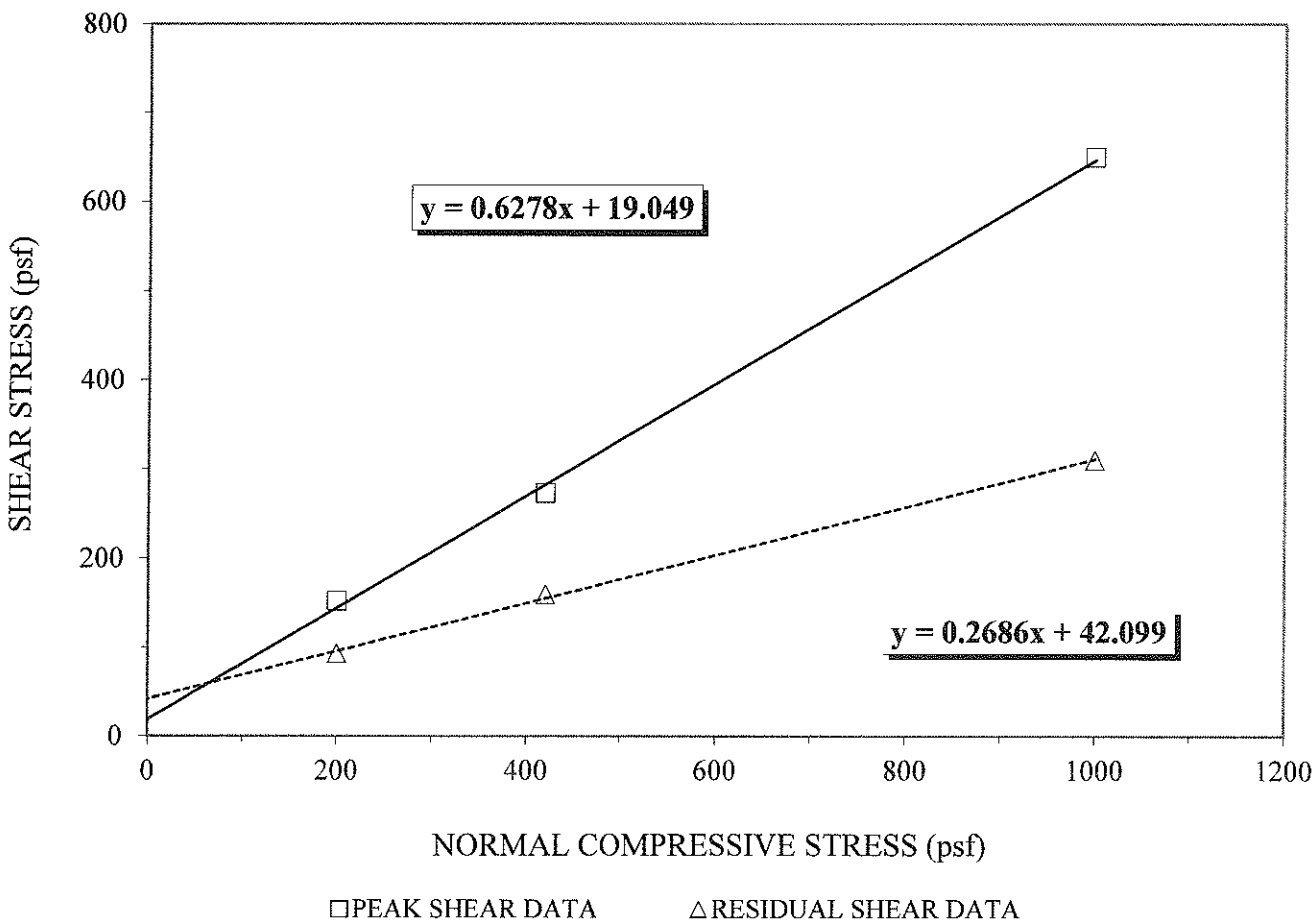




APPROVED BY : DATE : 6-10-14



544 Braddock Avenue • East Pittsburgh, PA 15112 • 412-823-7600 • FAX 412-823-8999 • www.geotechnics.net

REFERENCE 1-C

# INTERFACE FRICTION TEST RESULTS

## ASTM D 5321

geotechnics
INTEGRITY IN TESTING

CLIENT : King Construction Services, Inc.
CLIENT PROJECT : Horry County East Hill Closure
PROJECT NO. : L14061-01
LAB I. D. NO.: Skaps TN 300-2-6 Geocomposite (L14061-01-02)
Agru 40 mil LLDPE Microspike, Roll # 343519-11 (L14061-01-01)

INTERFACE : **Geocomposite**
**vs. 40 mil LLDPE Microspike (Bottom/Shiny Side)**

SHEAR RESISTANCE VS HORIZONTAL DISPLACEMENT

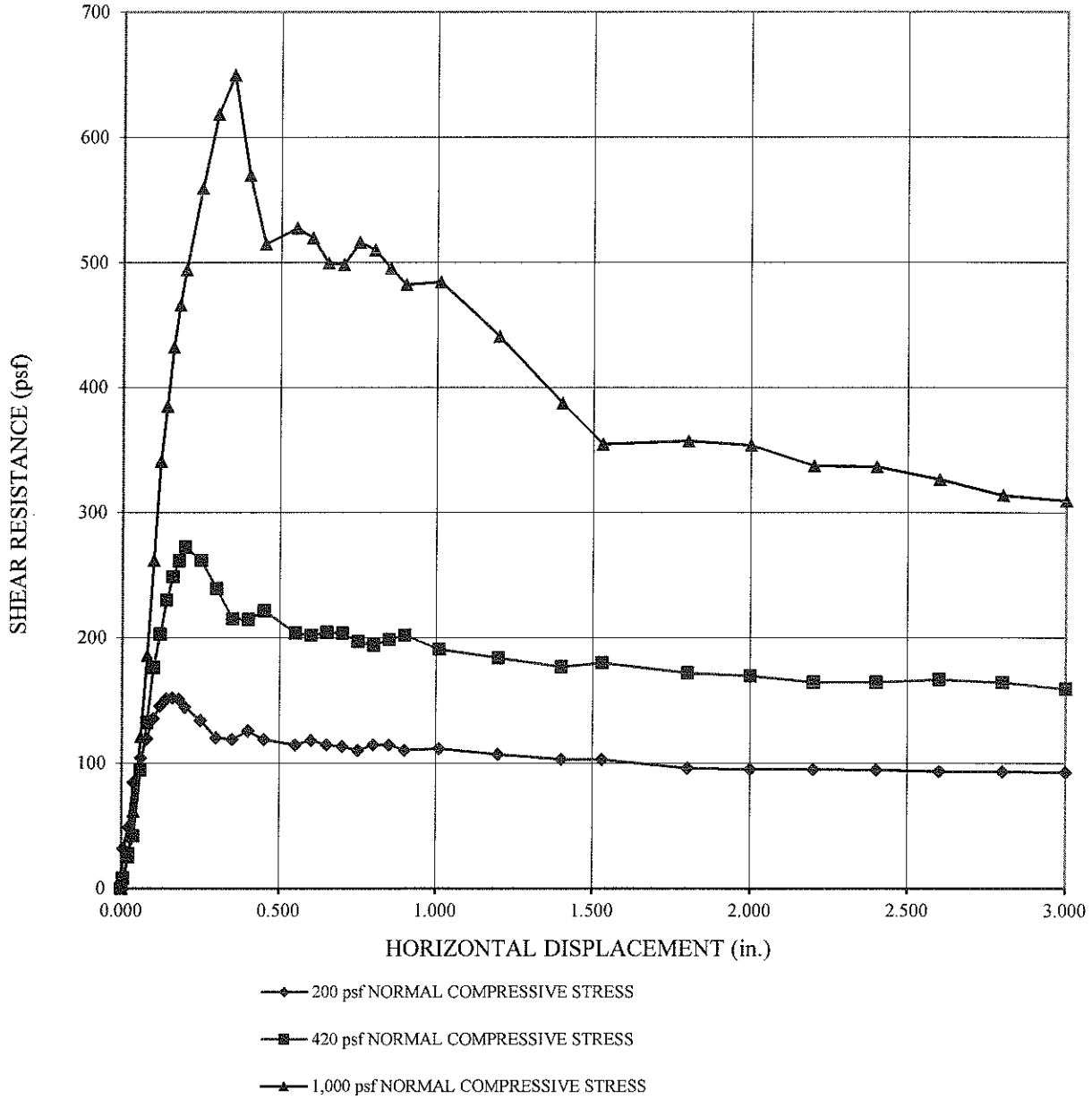




APPROVED BY : DATE : 6-10-14

\\geoserver\Data Drive\Ryan\Finished Reports\L14\061\01\[L14061-01 INT 2.xls]3 Points L14061-01 6/10/2014

544 Braddock Avenue • East Pittsburgh, PA 15112 • 412-823-7600 • FAX 412-823-8999 • www.geotechnics.net

REFERENCE 1-C

# INTERFACE FRICTION TEST RESULTS
## ASTM D 5321

geotechnics
INTEGRITY IN TESTING

CLIENT : King Construction Services, Inc.
CLIENT PROJECT : Horry County East Hill Closure
PROJECT NO. : L14061-01
LAB I. D. NO.S: Skaps TN 300-2-6 Geocomposite (L14061-01-02)
Agru 40 mil LLDPE Microspike, Roll # 343519-11 (L14061-01-01)

INTERFACE : **Geocomposite**
**vs. 40 mil LLDPE Microspike (Bottom/Shiny Side)**

STRAIN RATE ( in / min ) : 0.20 DIRECT SHEAR UNIT: LNL
PLACEMENT CONDITION: Inundated NORMAL LOAD: Platen Weight

| | | | | | | | | |
|---|---|---|---|---|---|---|---|---|
| NORMAL LOAD (psf) | | 200 | NORMAL LOAD (psf) | | 420 | NORMAL LOAD (psf) | | 1000 |
| PEAK SHEAR STRESS (psf) | | 152 | PEAK SHEAR STRESS (psf) | | 272 | PEAK SHEAR STRESS (psf) | | 650 |
| PEAK SECANT ANGLE (deg) | | 37.3 | PEAK SECANT ANGLE (deg) | | 33.0 | PEAK SECANT ANGLE (deg) | | 33.0 |
| RESIDUAL SHEAR (psf) | | 93 | RESIDUAL SHEAR (psf) | | 159 | RESIDUAL SHEAR (psf) | | 310 |
| RESID. SECANT ANGLE (deg) | | 24.9 | RESID. SECANT ANGLE (deg) | | 20.8 | RESID. SECANT ANGLE (deg) | | 17.2 |
| ASPERITY | | 30 | ASPERITY | | 31 | ASPERITY | | 31 |
| HORIZONTAL | | | HORIZONTAL | | | HORIZONTAL | | |
| DISPLACE. (in.) | SHEAR FORCE (lbs) | STRESS (psf) | DISPLACE. (in.) | SHEAR FORCE (lbs) | STRESS (psf) | DISPLACE. (in.) | SHEAR FORCE (lbs) | STRESS (psf) |
| 0.000 | 0 | 0 | 0.000 | 0 | 0 | 0.000 | 0 | 0 |
| 0.005 | 32 | 32 | 0.005 | 8 | 8 | 0.005 | 4 | 4 |
| 0.023 | 49 | 49 | 0.023 | 28 | 28 | 0.023 | 25 | 25 |
| 0.038 | 85 | 85 | 0.038 | 42 | 42 | 0.038 | 62 | 62 |
| 0.060 | 104 | 104 | 0.060 | 95 | 95 | 0.060 | 121 | 121 |
| 0.080 | 120 | 120 | 0.080 | 133 | 133 | 0.080 | 186 | 186 |
| 0.100 | 136 | 136 | 0.100 | 176 | 176 | 0.100 | 262 | 262 |
| 0.120 | 146 | 146 | 0.120 | 203 | 203 | 0.120 | 341 | 341 |
| 0.140 | 151 | 151 | 0.140 | 230 | 230 | 0.140 | 385 | 385 |
| 0.160 | 152 | 152 | 0.160 | 249 | 249 | 0.160 | 432 | 432 |
| 0.180 | 151 | 151 | 0.180 | 262 | 262 | 0.180 | 466 | 466 |
| 0.200 | 145 | 145 | 0.200 | 272 | 272 | 0.200 | 494 | 494 |
| 0.250 | 134 | 134 | 0.250 | 262 | 262 | 0.250 | 559 | 559 |
| 0.300 | 120 | 120 | 0.300 | 239 | 239 | 0.300 | 618 | 618 |
| 0.350 | 119 | 119 | 0.350 | 215 | 215 | 0.350 | 650 | 650 |
| 0.400 | 126 | 126 | 0.400 | 215 | 215 | 0.400 | 570 | 570 |
| 0.450 | 119 | 119 | 0.450 | 222 | 222 | 0.450 | 515 | 515 |
| 0.550 | 115 | 115 | 0.550 | 204 | 204 | 0.550 | 528 | 528 |
| 0.600 | 118 | 118 | 0.600 | 202 | 202 | 0.600 | 520 | 520 |
| 0.650 | 115 | 115 | 0.650 | 204 | 204 | 0.650 | 500 | 500 |
| 0.700 | 114 | 114 | 0.700 | 203 | 203 | 0.700 | 499 | 499 |
| 0.750 | 110 | 110 | 0.750 | 197 | 197 | 0.750 | 516 | 516 |
| 0.800 | 115 | 115 | 0.800 | 194 | 194 | 0.800 | 510 | 510 |
| 0.850 | 115 | 115 | 0.850 | 199 | 199 | 0.850 | 495 | 495 |
| 0.900 | 111 | 111 | 0.900 | 202 | 202 | 0.900 | 482 | 482 |
| 1.010 | 112 | 112 | 1.010 | 191 | 191 | 1.010 | 484 | 484 |
| 1.200 | 107 | 107 | 1.200 | 184 | 184 | 1.200 | 441 | 441 |
| 1.400 | 103 | 103 | 1.400 | 177 | 177 | 1.400 | 387 | 387 |
| 1.530 | 103 | 103 | 1.530 | 180 | 180 | 1.530 | 354 | 354 |
| 1.800 | 96 | 96 | 1.800 | 172 | 172 | 1.800 | 357 | 357 |
| 2.000 | 95 | 95 | 2.000 | 170 | 170 | 2.000 | 354 | 354 |
| 2.200 | 95 | 95 | 2.200 | 165 | 165 | 2.200 | 337 | 337 |
| 2.400 | 95 | 95 | 2.400 | 165 | 165 | 2.400 | 336 | 336 |
| 2.600 | 93 | 93 | 2.600 | 166 | 166 | 2.600 | 326 | 326 |
| 2.800 | 93 | 93 | 2.800 | 164 | 164 | 2.800 | 314 | 314 |
| 3.000 | 93 | 93 | 3.000 | 159 | 159 | 3.000 | 310 | 310 |


APPROVED BY : DATE : 6-10-14
\\geoserver\Data Drive\Ryan\Finished Reports\L14\061\01\[L14061-01 INT 2.xls]3 Points L14061-01 6/10/2014
544 Braddock Avenue • East Pittsburgh, PA 15112 • 412-823-7600 • FAX 412-823-8999 • www.geotechnics.net

REFERENCE 1-D

# A TECHNICAL NOTE REGARDING INTERPRETATION OF COHESION AND FRICTION ANGLE IN DIRECT SHEAR TESTS

There is often confusion expressed in the geosynthetics industry over how laboratory direct shear results should be interpreted, specifically whether one should use both the friction angle and cohesion (or adhesion) parameters. The attached technical note from the April/May 2009 issue of Geosynthetics provides some guidance regarding this question, as well as several other issues related to direct shear results.

Please note that this article is not intended to replace education or experience and should only be used in conjunction with professional judgment. In the end, all data should be evaluated by an experienced practitioner qualified to use the test results properly.

TR-264
05/14

847.851.1800 | 800.527.9948

© 2014 CETCO. IMPORTANT: The information contained herein supersedes all previous printed versions, and is believed to be accurate and reliable. For the most up-to-date information, please visit www.CETCO.com. CETCO accepts no responsibility for the results obtained throught application of this product. CETCO reserves the right to update information without notice.

TR_264_AM_EN_201405_v1

An AMCOL Company
www.CETCO.com

REFERENCE 1-D

# A technical note regarding interpretation of cohesion (or adhesion) and friction angle in direct shear tests

*By Richard Thiel*

## Introduction

Direct shear testing with geosynthetics is generally performed in accordance with ASTM D5321, *Standard Test Method for Determining the Coefficient of Soil to Geosynthetic or Geosynthetic to Geosynthetic Friction by the Direct Shear Method.* There is also a related standard, D6243, *Standard Test Method for Determining the Internal and Interface Shear Resistance of Geosynthetic Clay Liner by the Direct Shear Method.* This technical note applies to both equally.

## Interpreting lab results

There is often confusion expressed in the industry regarding how laboratory results should be interpreted, specifically: whether one should use both the friction angle and cohesion (or adhesion) parameters; whether cohesion should be ignored; whether secant friction angles are more appropriate; what to do if the data are nonlinear; and how the data should be interpolated or extrapolated.

The goal of this technical note is to provide some guidance to take the mystery out of these questions. In the end, all data should be evaluated by an experienced practitioner qualified to use the test results properly.

What this note will not do is go into the subtleties of requesting, setting up, calibrating, and performing a direct shear test. That would be the subject of additional articles.

| | |
|---|---|
| Material 1: | GSE 40 mil HDPE Tex / Tex (White side towards GCL) |
| Material 2: | Bentomat DN GCL (black side up) Roll # 00000481 |
| Substrate: | GSE 60 mil HDPE Tex-white / Tex-black (Black side toward GCL) |

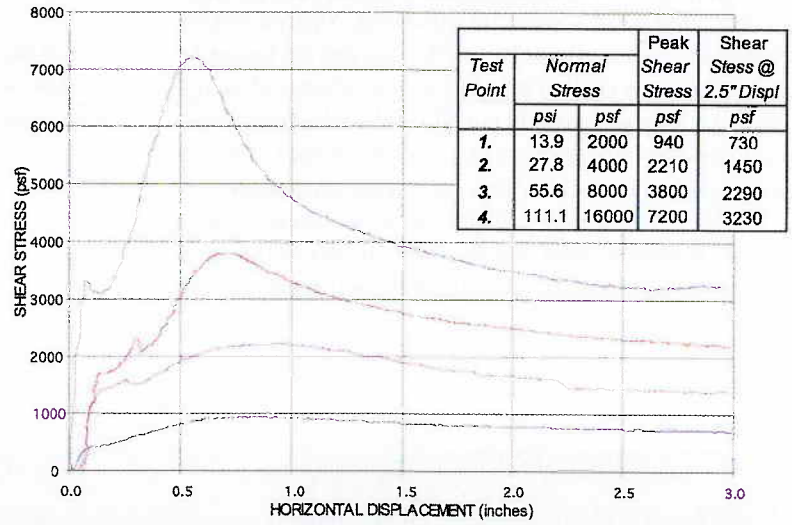


| Test Point | Normal Stress psi | Normal Stress psf | Peak Shear Stress psf | Shear Stess @ 2.5" Displ psf |
|---|---|---|---|---|
| 1. | 13.9 | 2000 | 940 | 730 |
| 2. | 27.8 | 4000 | 2210 | 1450 |
| 3. | 55.6 | 8000 | 3800 | 2290 |
| 4. | 111.1 | 16000 | 7200 | 3230 |

| |
|---|
| The "gap" between shear boxes was set at 80 mil (2.0 mm) |
| The test specimens were flooded during testing. |
| High Normal Stresses, >5psi (35 kPa) was applied using air pressure. |
| Low Normal Stresses, <5psi (35 kPa) was applied using dead weights. |
| The tests were terminated after 3.0"(75 mm) of displacement unless otherwise noted. |
| Tests were performed in general accordance with ASTM procedure D-5321 using a Brainard-Killman LG-112 direct shear machi |
| with an effective area of 12" x 12" (300 x300 mm). |
| Each specimen of 60 mil geomembrane was cut to 14" x 20" and clamped to the lower shear box. Avg. Asperity =0.025" |
| Each specimen of 40 mil geomembrane was cut to 14" x 16" and clamped to the upper shear box. Avg. Asperity =0.016" |
| Each GCL specimen was Hydrated for 48 hrs at the 250 psf, then placed, unclamped between upper & lower HDPEs |
| The grouped specimens were consolidated 16 hrs. under the specified normal stress, then sheared |
| Shearing occurred at the interface of the GCL's and 40 mil geomembrane specimens. |
| Extrusion of bentonite was noted on the surface of the 40 mil & white side of the GCL contact area for points 2,3 & 4 |
| The Friction Angle and Adhesion (or Cohesion) results given here are based on a mathematically determined best fit line. |
| Further interpretation should be conducted by a qualified professional experienced in geosynthetic and geotechnical engineering. |

This article will also not definitively describe how direct shear test data should be interpreted. That is the responsibility of a professional with specific expertise, and one article could never presume to cover all of the considerations that might apply to any unique design problem that might arise. That is why professionals are trained and mentored in basic geotechnical principles: so they can appropriately account for the various factors affecting a design and make appropriate decisions regarding test data interpretations.

The typical sequence of events related to direct shear testing includes the following:

**1.** An engineer requests a direct shear test series to obtain data to help solve a problem. The request should be very specific with regard to all the necessary details regarding

| Richard Thiel is a senior project manager at Vector Engineering Inc. in Grass Valley, Calif.

The Designer's Forum column is refereed by Greg Richardson, Ph.D., P.E., a principal at RSG & Associates, Raleigh, N.C., www.rsgengineers.com

REFERENCE 1-D

sampling, specimen preparation and setup in the testing device, and test execution in accordance with both project-specific conditions and industry standards.

**2.** A competent and certified laboratory performs the test series in accordance with the request and the industry standard test method (e.g., ASTM D5321 or D6243). The laboratory reports results to the engineer.

**3.** The engineer interprets and applies the results to the project design.

**What we are measuring in the direct shear test is shear strength as a function of normal load. The test does not measure "friction" or "cohesion," as these are simply mathematical parameters derived from the laboratory test results.**

Ideally the engineer who originally specified and required the shear test would be the same one who reviews and interprets the results. Sometimes, such as in a third-party construction quality assurance (CQA) project, an engineer other than the original designer will commission and review the testing. Interactions with test laboratories and other engineers over time have shown that there are often misconceptions and misunderstandings related to the interpretation of direct shear test data. Thus, this article is intended to serve the purpose of helping project participants avoid confusion. The key point of this article is that what we are measuring in the direct shear test is shear strength as a function of normal load. The test does not measure "friction" or "cohesion," as these are simply mathematical parameters derived from the laboratory test results.

**Figure 1** presents shear test results of a 4-point test for an interface between a textured geomembrane and a reinforced GCL. Three shear points, each at a different normal stress, are the most common number of points used to run a test series, but the number of points could vary from as few as one, to perhaps as many as six points, depending on many factors beyond the scope of this article. The figure shows: (a) a table of the normal stresses vs. peak and large-displacement shear strengths measured at 2.5in. of displacement, (b) graphs of the shear stress vs. displacement measurements, and (c) notes describing test conditions and observations.

There is adequate information in this figure for a trained practitioner to evaluate and use the data. The laboratory has performed its duty, which is to measure and report the shear strength under specified normal stresses (we are simplifying the dis-

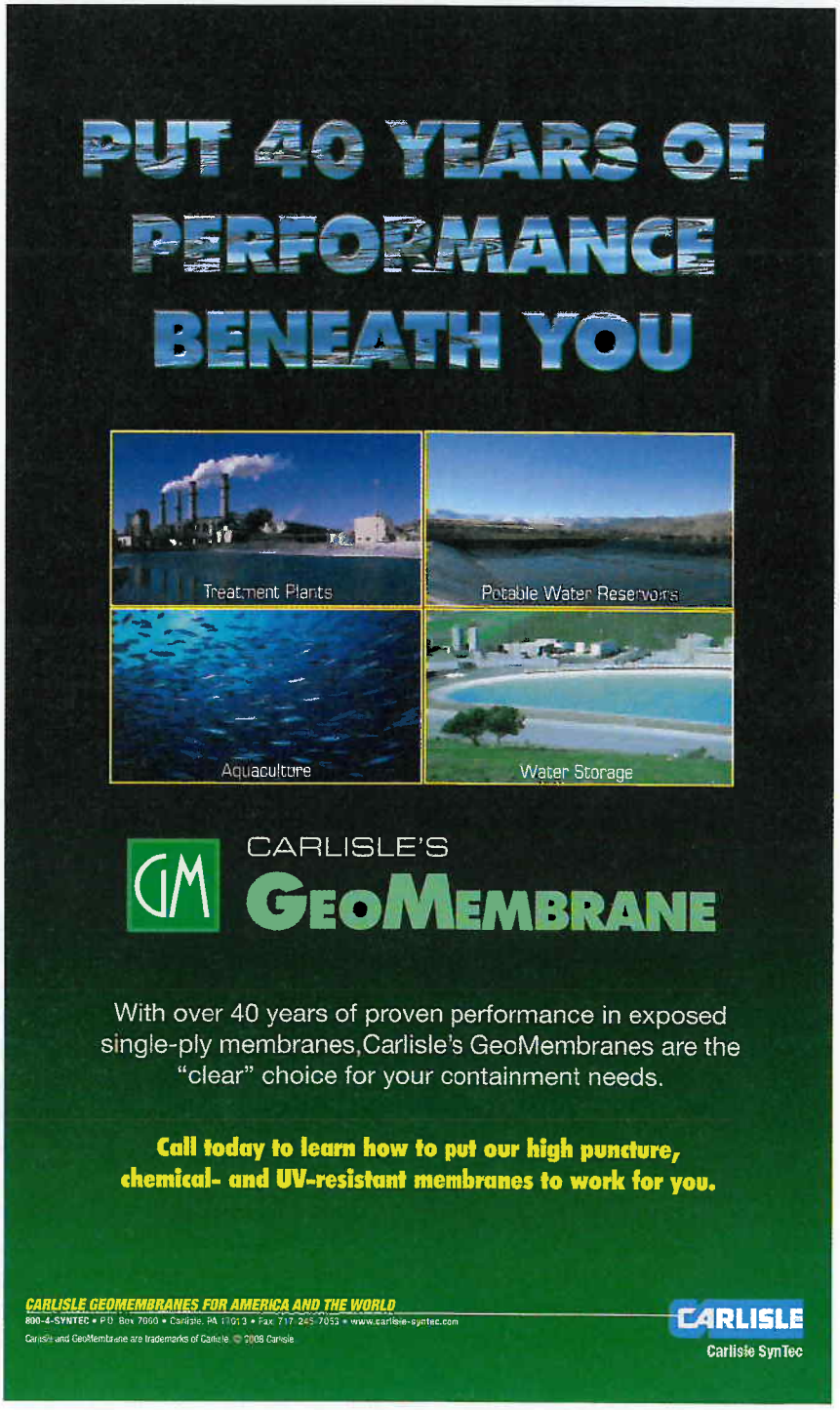

REFERENCE 1-D

cussion here by not elaborating on other factors such as hydration, consolidation, etc.), showing how the shear strength changed with displacement of the two surfaces, and providing descriptive and observational notes.

**Figure 2** shows additional information that can be provided by a laboratory in the form of a graph of the peak and large-displacement strengths plotted as a function of normal stress. Best-fit straight lines, called Mohr-Coulomb strength envelopes, named after the gentlemen who first publicized the relationship between shear strength and normal stress, have been drawn through the two sets (peak and large-displacement) of data points.

Equations can be written for these lines, as we learned in first-year algebra class, in the form of $y = mx + b$. In this case we define $y$ as the shear strength ($S$); $m$ as the slope of the line that we call the "coefficient of friction" and whose angle is *phi* ($\phi$), which we call the "friction angle" (and thus $\tan[\phi]$ is the slope of the line); $x$ is the normal stress ($N$); and $b$ is the y-intercept of the line that we call either "adhesion" ($a$, usually used for geosynthetics-only tests) or "cohesion" ($c$, usually used for tests involving soils, which will be used for the remainder of this article).

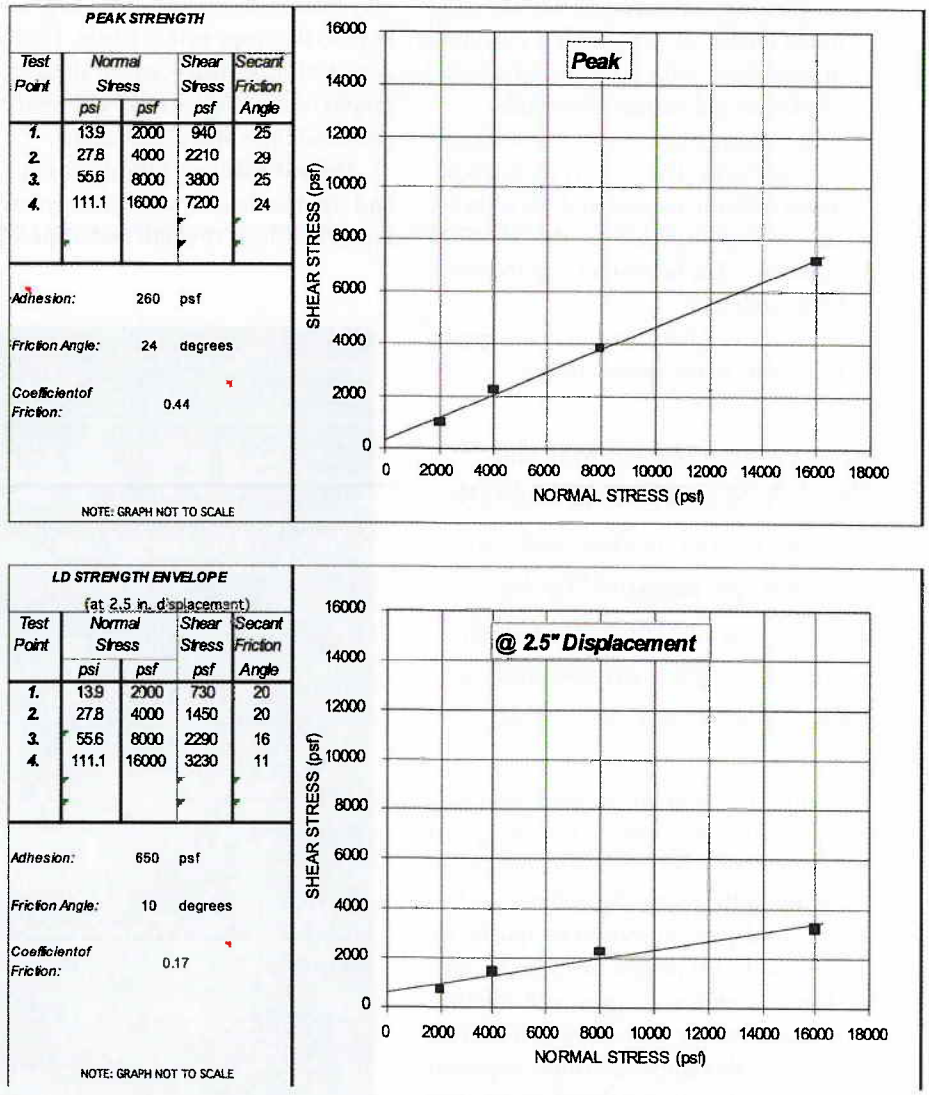


**Figure 2** | Example of supplemental data interpretation provided by the laboratory.

## Mohr-Coulomb

In geotechnical engineering, we write the Mohr-Coulomb equation for these lines as:

$$S = N \cdot \tan(\phi) + c$$

This equation is written for peak, large-displacement, or residual shear strength conditions. The fundamental points in this article regarding the presentation of the data in **Figure 2** include the following:

**1. The Mohr-Coulomb envelope should not be extrapolated beyond the limits of the normal stresses under which the testing was conducted.** To do so would never be conservative and, in fact, may be significantly nonconservative. The reason that simple extension-extrapolations of the Mohr-Coulomb envelope are nonconservative is presented in **Figure 3**. Most shear strength envelopes are truly curved (nonlinear). This tendency for a curved failure envelope is exaggerated in **Figure 3**, but can clearly be identified for the real-life strength envelopes presented in **Figure 2**, in particular for large-displacement conditions.

The Mohr-Coulomb model is merely a linear simplification of a portion of the entire envelope over a limited range of normal stresses. If testing were performed over a large enough range of normal stresses the curvature would become more apparent. True shear strength envelopes are found to be most accurately described by hyperbolic functions. Giroud et al. (1993) provides a good method to describe hyperbolic strength envelopes.

**2. The values of *phi* and *c* should be considered nothing more than mathematical parameters to describe the shear strength vs. normal stress *over the normal-load range the test was conducted.*** It is perhaps better not to think of "friction" and "cohesion" as real material properties, but simply as mathematical parameters to describe the failure envelope.

REFERENCE 1-D

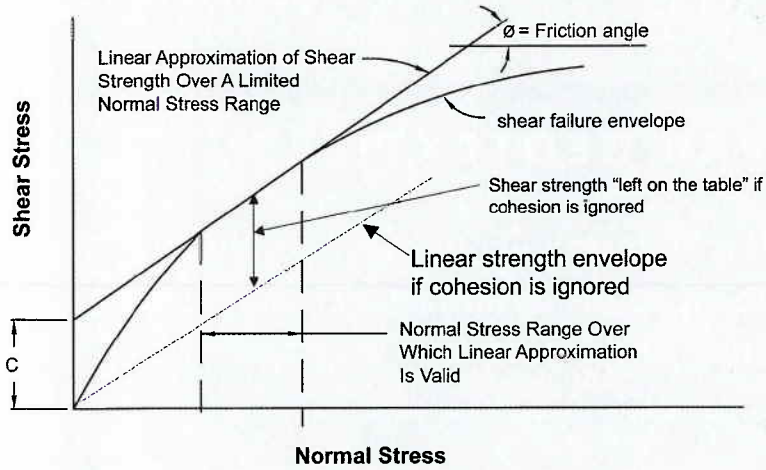


**Figure 3** | Exaggerated schematic of true curvilinear shear strength envelope, linear interpretation over a selected normal stress range, and the penalty for ignoring cohesion.

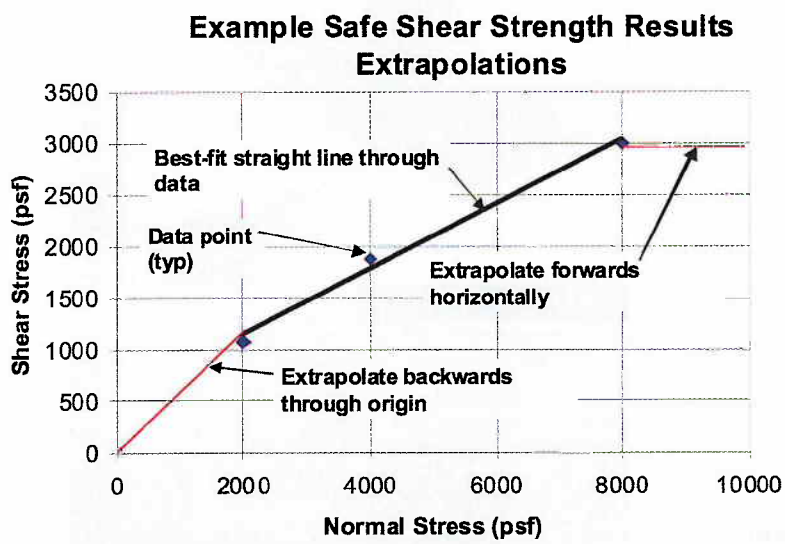


**Figure 4** | Example of safe shear strength extrapolation.

In geotechnical practice with soils, there are situations and examples where the cohesion parameter is evaluated separately from the friction parameter, but these are sophisticated considerations that involve very project-specific materials and conditions and should only be done by experienced professionals.

For many geosynthetic interfaces and in the context of many types of projects, there is absolutely no reason to dissociate the slope of the line from its y-intercept, and the shear strength should be taken as a whole in those cases. Other situations may occur, however, where it is appropriate, but those considerations are beyond the scope of this article.

**3.** In many, if not most, cases with geosynthetics where there is no reason to ignore the cohesion value, it is important to re-emphasize that shear strength should only be defined within the range of normal stresses for which the Mohr-Coulomb envelope was derived. Ignoring the cohesion may be unjustifiably penalizing the shear strength values that were measured in the test, as illustrated in **Figure 3**.

Using the cohesion value at normal stresses extrapolated below the range of testing, however, could have dire consequences on the safety of a design project. This problem may occur when designers consider only the operational or final build-out of a facility and they ignore the construction condition. Several failures have occurred during construction because of this. For example, an embossed geomembrane against a geotextile may perform well under high normal loads by providing a good friction angle and a modest y-intercept for operating and final build-out conditions. However, under the low normal loads experienced during construction of a thin soil veneer on a steep sideslope, testing might reveal that the adhesion extrapolated from the high-normal load results do not exist at low normal loads. In this case, a more aggressive texturing that exhibits a "Velcro®-effect" type of adhesion, or a very high friction angle, at low normal loads may be needed and should be verified at the proper normal loads.

**4. Figures 1** and **2** also report *secant* friction angles for each point. These are the angles of the straight lines from each point drawn back to the origin. A key concept regarding secant friction angles is that you should never extrapolate a secant angle line beyond the normal load for which it is measured. Secant values are conservative as long as the secant values are derived from a test whose normal stress was greater than the normal stresses of the design. They can quickly become nonconservative if the same friction angle is used for higher normal loads.

**5.** If users wish to extrapolate shear strength data, **Figure 4** illustrates the only "safe" way to accomplish this. Going from the low end of the Mohr-Coulomb envelope and extrapolating backward, the data can be extrapolated by drawing a straight line back to the origin. Going from the high end of the Mohr-Coulomb envelope and extrapolating forward, the data can be extrapolated by drawing a straight line

REFERENCE 1-D

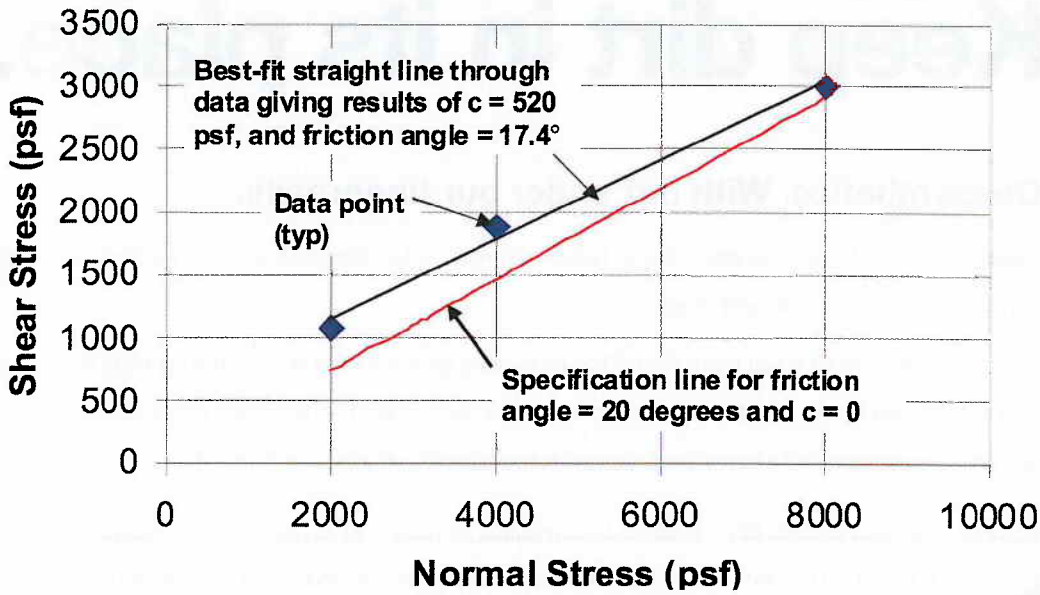


**Figure 5** | Example project results where interpretation of test data results in lower friction angle than specified value, even though shear strength results are higher than the failure envelope implied by the specifications.

horizontally forward. This extrapolation rule is safe only when considering a single interface. When multiple interfaces are involved, it is not safe to extrapolate a multi-layered system on the high side of the Mohr-Coulomb envelope.

From the discussion above, we can now look at the ASTM standard D5321 with more understanding and critical thought. The first thing to note is that the title of that standard is poorly worded. The title is "*Determining the Coefficient of…Friction…*" This is somewhat misleading because it implies that the designer is simply after a coefficient of friction. In fact, what designers need is a relationship between shear strength and normal stress. Therefore, a more appropriate title for this method would be "*Determining the Relationship between Shear Strength and Normal Stress for Soil-to-Geosynthetic or Geosynthetic-to-Geosynthetic Interfaces Using the Direct Shear Method.*" Note that ASTM D6243 has already rectified this problem in its title.

Another misleading element in ASTM D5321 is the definition of *adhesion* (which applies equally to cohesion), which it states as: "The shearing resistance between two adjacent materials *under zero normal stress* (emphasis added). Practically, this is determined as the y-intercept to a straight line relating the limiting value of shear stress that resists slippage between two materials and the normal stress across the contact surface of the two materials."

This is actually *two separate definitions,* which are most likely not the intent of the standard. The first part of this definition, which defines the adhesion as the shear strength at zero normal stress, is not applicable relative to the test method. It *could be true* if we proposed to test the interface at zero normal load, but that is rarely done and generally of no use. The industry would be better served by deleting the first part of the definition. In reality, the second part of the definition is the controlling aspect of the definition, and the "y-intercept" concept is the true nature of the adhesion value which, as stated above, is simply a mathematical parameter.

Note that ASTM D6243 has a different set of definitions, and it is not clear if those definitions are unique to that standard, or are intended to be industry norms. ASTM D6243 suggests that adhesion is the true shear strength when there is truly zero normal load, and that cohesion is the mathematical parameter of the y-intercept obtained from the Mohr-Coulomb envelope. In the author's opinion these definitions are acceptable as stated, but the audience should know that the definition of *adhesion* may conflict with other definitions put forward in the industry. Also, other authors have introduced other terms for the measurable shear strength under zero normal load, such as Lambe and Whitman's (1969) "*true cohesion.*" Interested readers can research ASTM D6243 and the literature and judge for themselves.

## Example problem 1

The following situation illustrates a common example of a problem that occurs with shear test data interpretation:

- A specification is written that requires a certain minimum interface friction angle to be achieved between a textured geomembrane and a GCL. For purposes of this example, the requirement is 20° peak shear strength for normal loads tested between 2,000 and 8,000 pounds per square foot (psf).
- The laboratory results, shown as an

REFERENCE 1-D

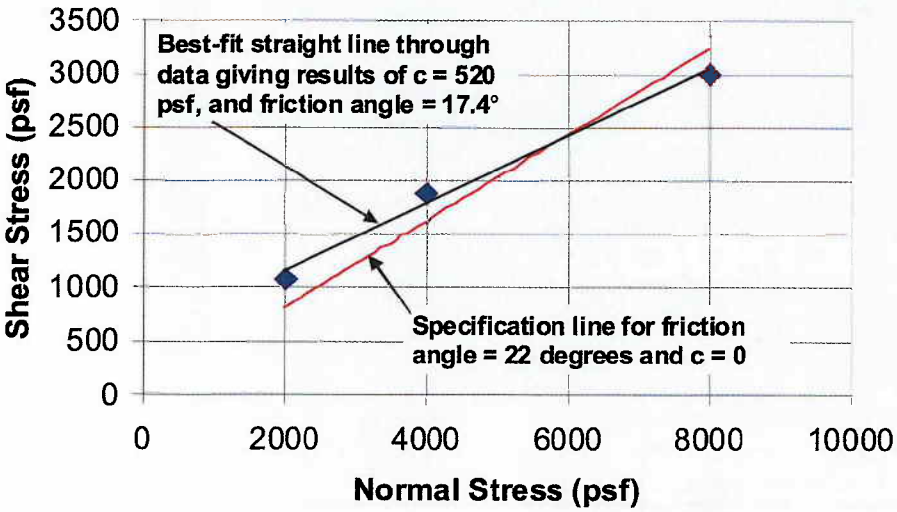


**Figure 6** | Example project results where the two lower points are above the specification and the upper point is below the specification.

example in **Figure 5**, report a best-fit Mohr-Coulomb peak strength envelope with shear strength parameters of 500 psf cohesion and 15° friction. **Figure 5** also shows the line representing the minimum project specification.

Inspection of **Figure 5** shows that the shear strengths achieved in the direct shear test plot above the shear strength envelope required by the specification. Even though the plot appears to clearly indicate that the minimum required shear strength is achieved by the products tested, the author has experienced several projects where one of the project parties (e.g., the design engineer or perhaps a regulator) have declared the test a failure because the reported Mohr-Coulomb friction angle was less than the specified friction angle.

In the author's opinion, in many cases involving this particular interface, there is no reason to consider this a failing test.

This example illustrates the confusion that might arise when specification is written in terms of a shear-strength *parameter*, when the real objective is to achieve a certain value of absolute shear strength. Even though the materials provided the shear strength required by the specification, there is some confusion because one of the strength *parameters* did not meet the specified value for that parameter.

It is possible that the original specifier had taken into account the potential for cohesion, and had wished to discount cohesion, and really wanted a true minimum friction angle of 20°. If the specifier were truly that sophisticated and had such complex reasoning, then more than likely the specification would have also been more sophisticated in explaining these constraints on the test results.

In the author's experience it is rare that other designers and specifiers are discounting cohesion with geosynthetic interfaces, and usually it is simply a matter of proper interpretation and communication of the design intent compared to the actual test results. Nevertheless, as stated at the beginning of this article, it is not the intent of this article to provide guidance and suggestions on interpreting test results. Rather, the intent is to shed light on some common misunderstandings.

## Example problem 2

The following problem has the same laboratory shear strength results as Problem 1, but the specification requirement is increased to 22° peak shear strength.

The relationship between the test results and the specification is shown in **Figure 6**. In this example, the two lower-normal load shear strength test results plot above the specification line, while the upper-normal load shear strength test result plots below the specification line. Based on the failing result of the upper-normal load test, most reviewers would initially say that this is a noncompliant test result and fails to meet the specification.

In the author's experience, curved failure envelopes are common, and the tendency for the highest normal-load result to fall beneath a straight-line friction-based specification is not unusual.

In this case, a more detailed review by the design engineer might reveal that the shear strength results provide an acceptable factor of safety for the intended purpose. It may be that the additional strength capacity provided in the lower normal load range that is above the specification more than offsets the reduced strength capacity in the upper normal load range that is below the specification. Clearly, the only person who can evaluate this issue, and who carries the requisite authority and responsibility, is the design engineer.

The following lessons can be gleaned from this example:

- Design engineers often attempt to specify a unique set of shear strength parameters as a minimum requirement for a given design. In reality, there may be an infinite combination of shear strength variations over the applicable range of normal loads that may satisfy the stability and shear resistance requirements, and many of these combinations may have a portion of their failure envelopes that fall below the specification.
- The tendency for natural and geosynthetic interfaces to yield curved failure envelopes can present a challenge to engineers, owners, and manufacturers who wish to optimize a design using simple straight-line shear strength specifications.
- A learned interpretation of direct shear testing data by an experienced practitioner may allow acceptance of apparently failing test results. This can occur because overly simplistic specification parameters may not ac-

REFERENCE 1-D

count for other combinations of shear strength results that could provide acceptable overall shear resistance.

## Summary

The direct shear test measures shear strengths as a function of normal stress. Period.

The test does not measure "friction angle" or "cohesion," as these values are parameters that are derived from the test results. Consideration of "friction angle" and "cohesion" simply as mathematical parameters used to describe shear strength data is of great benefit to practitioners for the following four reasons:

**1.** Interpretation of laboratory shear strength data should not be confused with the mathematical parameters used to describe it.

**2.** Proper data interpretation may avoid unnecessary penalization of the results by arbitrarily reducing the measured values.

**3.** This understanding can improve a designer's sensitivity to how important it is that shear strength is measured within the range of normal stresses that represent the design. Thus, the only defendable extrapolation of data should be: (a) back through the origin from the lowest normal stress, and (b) horizontally from the highest normal stress.

**4.** Laboratory shear strength data should be interpreted by a qualified practitioner experienced in the use and application of the results.

Often of much more importance than deciding whether to include or omit the cohesion (or adhesion) parameter is the decision of whether to use peak, post-peak, or residual shear strength. This discussion is beyond the scope of this technical note, and anyone commissioning and interpreting shear strength testing should be well versed in the issues surrounding this topic, as well.

**Acknowledgements**

The author would like to thank Richard Erickson and Chris Athanassopoulos for their review of this article.

**References**

Giroud, J.P., Darrasse, J., and Bachus, R.C., (1993). "Hyperbolic Expression for Soil-Geosynthetic or Geosynthetic-Geosynthetic Interface Shear Strength", *Geotextiles and Geomembranes*, Vol. 12, No.3, pp. 275–286.

Lambe, T.W. and Whitman, R.V., (1969). *Soil Mechanics*. John Wiley & Sons, New York, NY. G

Evolutionary Geomembrane development

New Elastoseal

**Trelleborg Elastoseal EPDM**
**with Thermobond thermofusion seaming**

**EPDM Rubber provides**
- Superior Durability and Service Life
- Superior Multidirectional Elasticity
- High Interface Friction
- Superior Substrate Conformance
- Installation at any temperature

**EPDM Rubber now also provides**
- Thermal Fusion Seaming for Factory and Field
- Conventional Air Channel QC Seam Testing
- Large Custom Prefabricated Panels

For more information,
visit www.trelleborg.com/rubber_membranes
or contact us on rubber.membranes@trelleborg.com

TRELLEBORG
BUILDING SYSTEMS

Trelleborg Building Systems AB, P.O.Box 1004, SE-331 29 Värnamo, Sweden
Tel: +46 370 481 00 Fax: +46 370 485 00

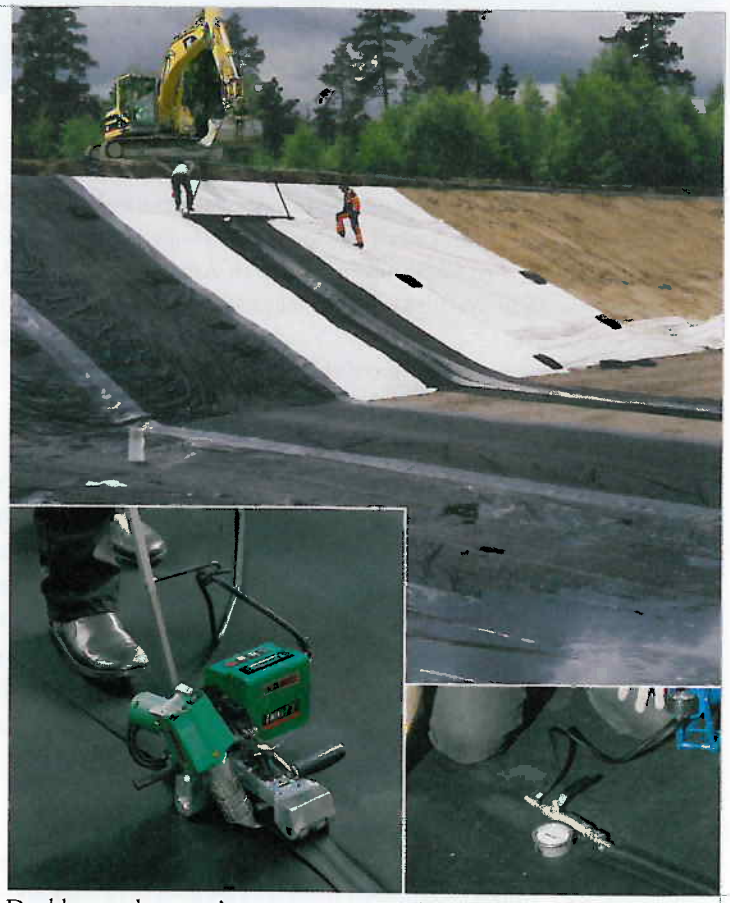

Dual hot wedge seaming  Air pressure testing

REFERENCE 1-E

Geosynthetics

# Static shear strength of geosynthetic clay liners

**Part 2: Static shear strength**

Geosynthetics | February 2013

By Chris Athanassopoulos, P.E. and Patrick Fox, Ph.D., P.E.

### Introduction

Part 2 of our three-part series on geosynthetic clay liner (GCL) shear strength is devoted to static shear strength, which is the strength measured for relatively slow loading conditions. Internal and interface static shear tests have been conducted for a wide range of GCL materials and normal stress conditions (Gilbert et al., 1996; Fox et al., 1998; Triplett and Fox, 2001; Chiu and Fox, 2004; Fox and Stark, 2004; Zornberg et al., 2005; McCartney et al., 2009; Fox and Ross, 2011). Part 2 presents some of this past research as well as new strength data obtained for ultra-high normal stress conditions. The focus is hydrated needlepunch-reinforced (NP) GCLs and their interface with textured high-density polyethylene (HDPE) geomembranes (GMXs), which are common liner materials, particularly in North and South America. Most of the test results presented herein were obtained using a large dynamic direct shear machine described by Fox et al. (2006). The main capabilities of this machine include a 305mm × 1067mm specimen size, a maximum normal stress of 2071 kPa, and a maximum shear displacement of 254mm. Subsequent modifications have made it possible to test specimens measuring 152mm × 1067mm, and thereby double the maximum normal stress to more than 4100 kPa. Although previously unnecessary, such high normal stress levels are becoming relevant for design of large facilities. Shear strength data presented in this article, as well as any other publications, are suitable only for preliminary design purposes. Final design values must always be measured using project-specific tests.

### GCL internal shear strength

Hydrated sodium bentonite has very low shear strength. For example, Fox et al. (1998) sheared a hydrated unreinforced GCL and reported a peak friction angle $\varphi_p = 10.2°$ and a residual friction angle $\varphi_r = 4.7°$. To increase the internal peak strength of a GCL, geosynthetic reinforcement is used to transmit shear stress across the weak hydrated bentonite layer. Reinforced GCLs can be manufactured as needlepunched or stitch-bonded. Needlepunching is now the preferred method and involves the use of barbed needles to pull nonwoven fibers from one geotextile through the bentonite core and the opposite geotextile. The industry uses the GCL peel strength index test (ASTM D6496) to assess the quality and strength of needlepunched reinforcement.

Figure 1 compares peak and residual failure envelopes for an unreinforced GCL, a stitch-bonded (SB) GCL, and two woven/nonwoven NP GCLs with different peel strengths($F_p$). The peak strength ($\tau_p$) envelopes indicate that reinforced GCLs are substantially stronger than unreinforced GCLs and that NP GCLs gain strength much faster than SB GCLs with increasing normal stress. The envelopes further indicate that higher peel strengths are associated with higher peak strengths for NP GCLs. Athanassopoulos and Yuan (2011) also found a correlation between peel strength and peak strength for a woven/nonwoven NP GCL. However, Zornberg et al. (2005) showed no clear trend between peel strengths and internal peak strengths for a large database of direct shear tests on the same type of NP GCL. Further work is needed to explain the inconsistency between these studies. The residual strength ($\tau_r$) envelopes in Figure 1 are the same for all types of GCLs because any reinforcement is ruptured by the time a GCL reaches the residual shear condition.

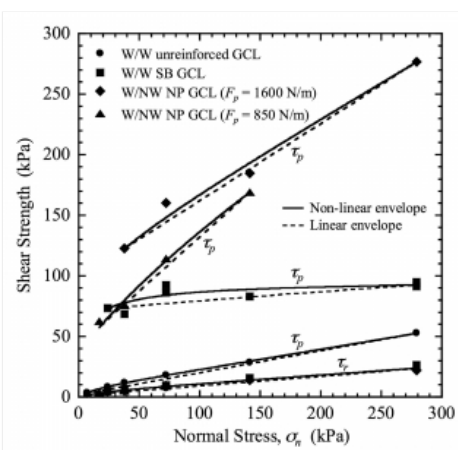


More recently, Fox and Ross (2011) performed a series of internal shear tests on a nonwoven/nonwoven NP GCL for normal stresses ranging from 71.9 kPa to 2071 kPa. This GCL contained 3.7 kg/m² of granular bentonite needlepunched between two 200 g/m² nonwoven geotextiles and had an average peel strength of 2170 N/m. The resulting internal peak and residual failure envelopes are shown in Figure 2.

REFERENCE 1-E

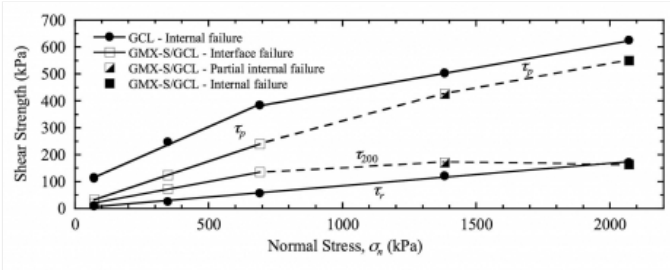


The peak envelope is bilinear and can be described by the following regression equations:

$\tau_p$ (kPa) = 83.7 kPa + $\sigma_n$ tan 23.7° (71.9 ≤ $\sigma_n$ ≤ 692 kPa)
$\tau_p$ (kPa) = 261.2 kPa + $\sigma_n$ tan 9.9° (692 ≤ $\sigma_n$ ≤ 2071 kPa)

Secant friction angles, defined as $\varphi_{sec}$ = arctan($\tau$/ $\sigma_n$) , provide additional perspective on the variation of shear strength with changing normal stress. In this case, internal peak secant angles decreased from 57.6° at $\varphi_n$ = 71.9 kPa to 16.8° at $\varphi_n$ = 2071 kPa. The internal residual shear strength envelope is linear and is described by:

$\tau_r$ (kPa) = 1.3 kPa + $\sigma_n$ tan 4.8° (71.9 ≤ $\sigma_n$ ≤ 2071 kPa)

Corresponding internal residual secant angles decreased from 7.8° at $\sigma_n$ = 71.9 kPa to 4.7° at $\sigma_n$ = 2071 kPa. These values are consistent with Figure 1 and indicate that little to no NP reinforcement remains intact after 200 mm of shear displacement.

### GMX/GCL interface shear strength

GMX/NP GCL interface shear tests have been performed by various researchers (Gilbert et al., 1996; Triplett and Fox, 2001; Chiu and Fox, 2004; Vukelic et al., 2008; McCartney et al., 2009). General findings from this work show that peak shear strengths for GMX/NP GCL interfaces are lower than for NP GCLs at low to moderate normal stress conditions. Additionally, peak interface strengths for a GMX placed against the nonwoven side of a NP GCL are higher than those for the woven side due to extrusion of hydrated bentonite through the woven geotextile. The quantity of extruded bentonite typically increases with increasing normal stress and is greater when a GCL is hydrated under low normal stress conditions.

Fox and Ross (2011) also completed a series of interface shear tests between a GMX and the same nonwoven/nonwoven NP GCL as previously discussed. The GMX was a 1.5mm-thick HDPE geomembrane with structured texturing and an average asperity height of 0.72 mm. Results are presented in Figure 2. The peak strength failure envelope is described by:

$\tau_p$ (kPa) = 8.2 kPa + $\sigma_n$ tan 18.4° (71.9 ≤ $\sigma_n$ ≤ 692 kPa)

Corresponding interface peak secant angles decreased from 24.1° at $\varphi_n$ = 71.9 kPa to 14.9° at $\varphi_n$ = 2071 kPa. At low normal stress, the large displacement (200mm) envelope is described by:

$\tau_{200}$ (kPa) = 7.3 kPa + $\sigma_n$ tan 10.5° (71.9 ≤ $\sigma_n$ ≤ 692 kPa)

Residual secant angles decreased from 15.5° at $\sigma_n$ = 71.9 kPa to 4.5° at $\sigma_n$ = 2071 kPa. With increasing normal stress above 692 kPa, the failure mode transitioned from the GMX/GCL interface to GCL internal, and both the peak and large displacement envelopes became nonlinear. Partial internal failure occurred at 1382 kPa and complete internal failure occurred at 2071 kPa. As a result, the residual shear strength of the GMX/GCL interface test at 2071 kPa was equal to that of the GCL internal test because the NP reinforcement of the GCL was completely ruptured after 200mm of displacement.

The nonlinear failure envelopes in Figure 2 provide another example illustrating that linear extrapolation of measured data above or below the tested range of normal stress may overestimate shear strength and should not be attempted. Similar recommendations have been made by Thiel (2009) and others.

### Failure mode transition

At high normal stress, the interface strength between a GMX and a NP GCL can exceed the strength of the needlepunched reinforcement and failure of a GMX/NP GCL composite liner system can occur internally within the GCL. The critical normal stress associated with this failure mode transition depends on the specific materials (e.g., GCL peel strength, GMX texturing and asperity height) and testing conditions (e.g., hydration/consolidation, displacement rate) and, as such, can vary over a wide range. Triplett and Fox (2001) observed no GCL internal failures for GMX/NP GCL interface tests conducted at normal stresses as high as 486 kPa. McCartney et al. (2009) likewise reported no GCL internal failures in a database of 534 geomembrane/GCL interface tests performed at normal stresses as high as 965 kPa. Similarly, Athanassopoulos et al. (2009) did not observe GCL internal failure until the normal stress reached 2759 kPa. The variability of normal stress at failure mode transition highlights the need for project-specific shear tests using representative materials and conditions. Observations of internal shear failure of NP GCLs are thus far limited to the laboratory because there are no known cases of internal shear failure of NP GCLs in the field (Fox and Ross, 2011; Koerner, 2012). Nonetheless, the potential for both interface and internal failure should be considered for designs that subject hydrated NP GCLs to high normal stress levels.

### Shear strength at ultra-high normal stress

Athanassopoulos et al. (2012) and Thielmann et al. (2013) evaluated GMX/NP GCL interface strengths for normal stresses as high as 4144 kPa. The NP GCL contained 3.7 kg/m$^2$ of granular bentonite needlepunched between two 200 g/m$^2$ nonwoven geotextiles and

REFERENCE 1-E

had an average peel strength of 2224 N/m. The GMX was a 1.5mm-thick HDPE geomembrane with co-extruded texturing and asperity heights ranging from 0.51 to 0.58 mm. Two sets of tests were conducted: (1) GMX/NP GCL interface tests with the materials placed between rigid backing plates; and (2) GMX/NP GCL interface tests with the materials placed between a lower layer of sand and an upper layer of coarse gravel, to better replicate common field conditions. For the first test series, interface peak secant angles decreased from 21.6° at 348 kPa to 13.4° at 4144 kPa, and corresponding interface large displacement secant angles decreased from 7.1° to 3.5°. Internal GCL failures were observed for normal stress levels of 2072 kPa and above. Interestingly, as shown in Figure 3, repeating these tests with the GMX/NP GCL liner system placed between soil layers produced modest increases (up to 8.5%) in peak shear strength and dramatic increases (up to 83%) in large displacement shear strength.

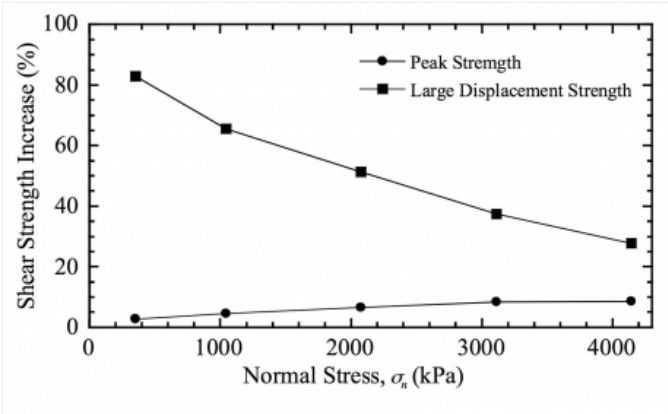


The increase in strength is due to local out-of-plane deformation, or "dimpling," of the liner components under the gravel particles, similar to those observed by Breitenbach and Swan (1999) and Parra et al. (2010). These results suggest that the common practice of performing direct shear tests using rigid backing plates is conservative with regard to shear strength of GMX/GCL composite liners that are overlain by gravelly soils.

**Summary and final comments**

High quality data on static shear strengths of GCLs and GCL interfaces are needed for stability analyses of liner systems that incorporate these unique materials. The following conclusions are based on the foregoing review of selected research on this topic:

- Reinforced GCLs are substantially stronger than unreinforced GCLs. NP GCLs gain strength much faster with increasing normal stress than SB GCLs. Higher peel strengths are often associated with higher peak strengths for NP GCLs.
- Peak shear strengths for a GMX interface with the nonwoven side of a NP GCL are consistently higher than those for the woven side. The quantity of bentonite extruded to the interface typically increases with increasing normal stress and is less for nonwoven geotextiles than for woven geotextiles.
- Peak shear strengths for GMX/NP GCL interfaces are generally lower than for NP GCLs at low to moderate normal stress conditions.
- GMX/NP GCL interfaces can experience GCL internal failure at high normal stress. The critical normal stress at which such failure mode transition occurs is highly dependent on the specific materials and testing conditions, and has been shown to range from 692 to 2759 kPa in recent studies.
- Internal failures of NP GCLs have thus far been observed only in the laboratory. Fox and Ross (2011) and Koerner (2012) report that there are no known cases of internal shear failure of NP GCLs in the field. Nonetheless, the potential for both interface and internal failure should be considered for designs that subject hydrated NP GCLs to high normal stress levels.
- The widespread practice of conducting direct shear tests on single interfaces with rigid backing plates appears to be conservative with regard to shear strength, and especially large displacement shear strength, of GMX/GCL composite liners that are overlain by gravelly soils.
- The variability of static shear strengths of GCLs and GCL interfaces highlights the need for project-specific shear tests using representative materials and conditions.

Part 3 will conclude this series with a discussion of the dynamic shear strength of GCLs. This emerging area of research is an important consideration for GCL liner systems subject to earthquakes and other dynamic loadings.

Chris Athanassopoulos, technical manager, CETCO, Hoffman Estates, Ill.; chris.athanassopoulos@amcol.com
Patrick Fox, professor, University of California-San Diego, La Jolla, Calif.; pjfox@ucsd.edu

Acknowledgements

Some of the data presented in this paper was obtained with funding provided by Grant No. CMMI-0800030 from the Geotechnical Engineering Program of the U.S. National Science Foundation and by CETCO of Hoffman Estates, Ill. This support is gratefully acknowledged.

References

REFERENCE 1-E

ASTM D6496. Standard Test Method for Determining Average Bonding Peel Strength between the Top and Bottom Layers of Needle-Punched Geosynthetic Clay Liners. ASTM International, West Conshohocken, Pa.

Athanassopoulos, C., Kohlman, A., Henderson, M., Kaul, J., and Boschuk, J. (2009). "Permeability, Puncture, and Shear Strength Testing of Composite Liner Systems under High Normal Loads," *Tailings and Mine Waste*.

Athanassopoulos, C., and Yuan, Z. (2011). "Correlation between Needlepunch-Reinforced Geosynthetic Clay Liner Peel Strength and Internal Shear Strength," *GeoFrontiers*, Dallas, Texas.

Athanassopoulos, C., Fox, P. J., and Thielmann, S. S. (2012). "Interface Shear Strength Testing of Geomembrane/GCL Composite Liner Systems under Ultra-High Normal Stresses," *EuroGeo5*, Valencia, Spain (CD-ROM).

Breitenbach, A. J., and Swan, R. H. (1999). "Influence of High Load Deformations on Geomembrane Liner Interface Strengths," *Geosynthetics '99*, 1, 517-529.

Fox, P. J., and Ross, J. D. (2011). "Relationship between GCL Internal and GMX/GCL Interface Shear Strengths," *Journal of Geotechnical and Geoenvironmental Engineering*, 137(8), 743-753.

Fox, P. J., Nye, C. J., Morrison, T. C., Hunter, J. G., and Olsta, J. T. (2006). "Large Dynamic Direct Shear Machine for Geosynthetic Clay Liners," *Geotechnical Testing Journal*, 29(5), 392-400.

Fox, P. J., Rowland, M. G., and Scheithe, J. R. (1998). "Internal Shear Strength of Three Geosynthetic Clay Liners," *Journal of Geotechnical and Geoenvironmental Engineering*, 124(10), 933-944.

Gilbert, R. B., Fernandez, F., and Horsfield, D. W. (1996). "Shear Strength of a Reinforced Geosynthetic Clay Liner," *Journal of Geotechnical Engineering*, 122(4), 259-266.

Koerner, R. M. (2012). "Selected Topics on Geosynthetic Clay Liners," Keynote Lecture, *GCL University*, CETCO, Washington, D.C., April.

McCartney, J. S., Zornberg, J. G., Swan, R. H., Jr. (2009). "Analysis of a Large Database of GCL-Geomembrane Interface Shear Strength Results," *Journal of Geotechnical and Geoenvironmental Engineering*, 135(2), 209-223.

Parra, D., Soto, C., and Valdivia, R. (2010). "Soil Liner-Geomembrane Interface Shear Strength using Rigid Substrata or Overliner," *9th International Conference on Geosynthetics*, Guaruja, Brazil. (CD-ROM).

Thiel, R. S. (2009). "Cohesion (or Adhesion) and Friction Angle in Direct Shear Tests: A Technical Note Regarding Interpretation of Cohesion (or Adhesion) and Friction Angle in Direct Shear Tests," *Geosynthetics*, April.

Thielmann, S. S., Fox, P. J., and Athanassopoulos, C. (2013). "Interface Shear Testing of GCL Liner Systems for Very High Normal Stress Conditions," *GeoCongress*, ASCE, in press.

Triplett, E. J., and Fox, P. J. (2001). "Shear Strength of HDPE Geomembrane/Geosynthetic Clay Liner Interfaces," *Journal of Geotechnical and Geoenvironmental Engineering*, 127(6), 543-552.

Vukelic, A., Szavits-Nossan, A., and Kvasnicka, P. (2008). "The Influence of Bentonite Extrusion on Shear Strength of GCL/Geomembrane Interface," *Geotextiles and Geomembranes*, 26, 82-90.

Zornberg, J. G., McCartney, J. S., and Swan, R. H. (2005). "Analysis of a Large Database of GCL Internal Shear Strength Results," *Journal of Geotechnical and Geoenvironmental Engineering*, 13 (3), 367-380.

### Comments

There are not yet any comments.

Copyright ©2015 Industrial Fabrics Association International. All rights reserved.

REFERENCE 2

Fourth Edition

# Designing with Geosynthetics

Robert M. Koerner, Ph.D., P.E.

H. L. Bowman Professor of Civil Engineering,
Drexel University and Director, Geosynthetic
Research Institute

PRENTICE HALL
Upper Saddle River, New Jersey 07458

REFERENCE 2

is its thickness, which can be determined using ASTM D1777. While there is no listing as such, it is recommended that geonet thickness be measured under a normal pressure of 420 lb./ft.$^2$ (20 kPa). This is the same pressure that is recommended to measure geomembrane thickness. Geonets are not nearly as sensitive to thickness variation under normal pressure as are geotextiles and are similar to geomembranes in this regard.

Mass per unit area can be determined using ASTM D1910. For a 200-mil (5.1-mm)-thick, extruded, solid-rib geonet, the mass per unit area is usually in the range of 20 to 30 oz./yd.$^2$ (680 to 1020 g/m$^2$). It is not a design property per se, but it is informative from a manufacturer's point of view.

Other physical properties such as rib dimensions, planar angles made by the intersecting ribs, vertical angles made at the juncture locations, aperture size and shape, etc., can be measured directly and are relatively straightforward to obtain.

### 4.1.2 Mechanical Properties

A number of various strength properties of geonets are important to consider.

**4.1.2.1 Tensile Strength** The wide-strip tensile strength of geonets is sometimes called for in various specifications. Using ASTM D4595, which uses a test specimen 8.0 in. (200 mm) in width by 4.0 in. (100 mm) in length, the curves of Figure 4.4 resulted in a 200-mil (5.1-mm)-thick solid rib extruded geonet in the machine and cross-machine directions. Note the differences in behavior, suggesting that there is a preferential direction in strength between the machine and cross-machine directions. If site-specific conditions warrant a high-strength direction, the geonet should be oriented with its machine direction positioned accordingly. Also to be noted is that geonets do indeed possess a measurable tensile strength. For the solid rib geonet illustrated in Figure 4.2 and shown in Figure 4.4, the average of a series of wide-strip tensile tests gave the following information:

- Machine direction:
  Peak strength = 680 lb./ft. (120 kN/m)
  Strain at peak = 23%
  Strain at failure = 290%
- Cross-machine direction:
  Peak strength = 390 lb./ft. (68 kN/m)
  Strain at peak = 170%
  Strain at failure = 240%

**4.1.2.2 Compressive Strength** Of greater importance than the aforementioned in-plane tensile strength of geonets is the cross-plane compressive strength. This is due to the influence that compressive yielding or collapse has on the ability of the geonet to conduct liquid within its planar structure. There are a number of approaches to measuring a geonet's compressive strength, and ASTM has a task committee working on the topic. Using 6.0-in. (150-mm)-square test specimens normally loaded under a constant strain rate load of 0.002 in./min. (= 0.05 mm/

## 2.4 ALLOWABLE VERSUS ULTIMATE GEOTEXTILE PROPERTIES

REFERENCE 2

Many of the preceding geotextile test properties represent ideal conditions and thereby result in high numeric values when used directly in design (i.e., they result in upper-bound values). In the design-by-function concept described in Section 2.1.3, the global factor of safety was formulated around on allowable test value (recall Equations 2.2a and 2.2b). Thus often the particular value cannot be used directly from the laboratory test and must be suitably modified for *in situ* conditions. This could be done directly in the test procedure (i.e., by conducting a completely simulated performance test); but in many cases it simply is not possible. Such situations as full-size test specimens, long-term creep testing, use of site-specific liquids, representation of *in situ* pore water stresses, complete stress state modeling, etc., are generally not feasible for laboratory situations. To account for the difference between the laboratory-measured test value and the desired performance value, two approaches can be taken:

1. Use an extremely high global factor of safety at the end of a problem.
2. Use partial factors of safety on the laboratory-generated test value to make it into a site-specific allowable value.

The latter alternative will be used in this book. By doing this, the usual global factor of safety value can be considered in the final analysis.

The approach taken will be to refer to the general laboratory-obtained value as an ultimate value and to modify it by partial factors of safety to an allowable value. For problems dealing with geotextile strength, the formulation takes the following form, with typical values given in Table 2.12. Note that these values, however, must be tempered by the site-specific considerations.

$$T_{\text{allow}} = T_{\text{ult}}\left(\frac{1}{FS_{ID} \times FS_{CR} \times FS_{CD} \times FS_{BD}}\right) \tag{2.24}$$

where $T_{\text{allow}}$ = the allowable tensile strength,
$T_{\text{ult}}$ = the ultimate tensile strength,
$FS_{ID}$ = the factor of safety for installation damage,
$FS_{CR}$ = the factor of safety for creep,
$FS_{CD}$ = the factor of safety for chemical degradation, and
$FS_{BD}$ = the factor of safety for biological degradation.

**Table 8.17 Various design models for geomembranes in waste disposal situations (after Richardson and Koerner [69])**

REFERENCE 2

| Problem | Liner Stress | Free Body Diagram | Required Properties: Geomembrane | Required Properties: Landfill | Typical Factor of Safety |
|---|---|---|---|---|---|
| 1. Liner self-weight | Tensile | 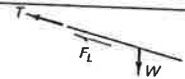 | $G$, $t$, $\sigma_{allow}$, $\delta_L$ | $\beta$, $H$ | 10 to 100 |
| 2. Weight of filling | Tensile | 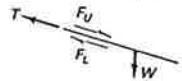 | $t$, $\sigma_{allow}$, $\delta_U$, $\delta_L$ | $\beta$, $h$, $\gamma$, $H$ | 0.5 to 10 |
| 3. Impact during construction | Impact | 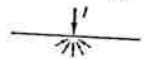 | $I$ | $d$, $W$ | 0.1 to 5 |
| 4. Weight of landfill | Compression | 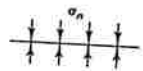 | $\sigma_{allow}$ | $\gamma$, $H$ | 10 to 50 |
| 5. Puncture | Puncture | | $\sigma_p$ | $\gamma$, $H$, $P$, $A_p$ | 0.5 to 10 |
| 6. Anchorage | Tensile | 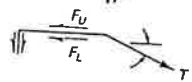 | $t$, $\sigma_{allow}$, $\delta_U$, $\delta_L$ | $\beta$, $\gamma$, $\phi$ | 0.7 to 5 |
| 7. Settlement of landfill | Shear | 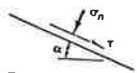 | $\tau$, $\delta_U$ | $\beta$, $\gamma$, $H$ | 10 to 100 |
| 8. Subsidence under landfill | Tensile | 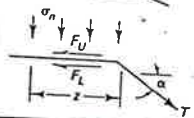 | $t$, $\sigma_{allow}$, $\delta_U$, $\delta_L$, $\chi$ | $\alpha$, $\gamma$, $H$ | 0.3 to 10 |

*Notes*:

- Geomembrane Properties
  - $G$ = specific gravity
  - $t$ = thickness
  - $\sigma_{allow}$ = allowable strength (yield, break, or allow)
  - $\tau$ = shear strength
  - $I$ = impact resistance
  - $\sigma_p$ = puncture strength
  - $\delta_U$ = friction with material above
  - $\delta_L$ = friction with material below
  - $\chi$ = mobilization distance
- Landfill Properties
  - $\beta$ = slope angle
  - $H$ = landfill height
  - $\gamma$ = unit weight
  - $h$ = lift height
  - $\alpha$ = subsidence angle
  - $\phi$ = friction angle
  - $d$ = drop height
  - $W$ = weight
  - $p$ = puncture force
  - $A_p$ = puncture area

REFERENCE 3

IN-LINE PLASTICS, LC

# HERCULINE SPECIFICATIONS
## HDPE Smooth

Herculine High Density Polyethylene is produced from virgin polyethylene resins. Herculine HDPE has outstanding chemical resistance, mechanical properties, environmental stress crack resistance, dimensional stability, and thermal aging characteristics. Herculine HDPE contains approximately 97.5% polymer and 2.5% carbon black, antioxidants and heat stabilizers, and contains no other additives, fillers or extenders. Herculine HDPE has excellent UV resistance. Herculine HDPE does not contain plasticizers which can migrate to the surface, causing premature aging. Manufactured from virgin polyethylene resins, it is designed to provide a high quality, economical geomembrane.

| Properties | Test Method | Typical Average Roll Values | | | |
|---|---|---|---|---|---|
| Color | | Black | Black | Black | Black |
| Thickness, mils – (min. ave.) | ASTM D5199 | 12 | 20 | 30 | 40 |
| • Lowest individual | | -15% | -10% | -10% | -10% |
| Density, gram/cm$^3$ - (min.) | ASTM D1505 | .94 | .94 | .94 | .94 |
| Tensile Properties – Each Direction | | | | | |
| Tensile Strength at Break, lbs/in width (N/mm) | ASTM D6693 Type IV | 43 (7) | 76 (13) | 114(20) | 152(27) |
| Tensile Strength at Yield, lbs/in width (N/mm) | Dumbell, 2 ipm | 23 (4) | 42 (7) | 63 (11) | 84 (15) |
| Elongation at Break, % | G.L. 2.0 in | 700 | 700 | 700 | 700 |
| Elongation at Yield, % | G.L. 1.3 in | 12 | 12 | 12 | 12 |
| Tear Resistance, lbs. (N ) | ASTM D1004 | 7 (33) | 13 (59) | 21 (93) | 28(125) |
| Puncture Resistance, lbs. (N) | ASTM D4833 | 19(86) | 34(152) | 54(240) | 72(320) |
| Carbon Black, % (min.) | ASTM D1603 | 2 | 2 | 2 | 2 |
| Carbon Black Dispersion | ASTM D5596 | Note (1) | Note (1) | Note (1) | Note (1) |

Note 1: 9 of 10 views shall be category 1 or 2. No more than 1 view from category 3.

*This data is provided for informational purposes only. In-Line Plastics, LC makes no warranties as to the suitability or the fitness for a specific use or merchantability of products referred to, no guarantee of satisfactory results from reliance upon contained information or recommendations and disclaims all liability from resulting loss or damage. This information is subject to change without notice, please check with In-Line Plastics for current updates.*

REFERENCE 3

## Geotextile Product Description Sheet

# SKAPS GE-110
# 10 oz Nonwoven Geotextile

SKAPS GE-110 is a needle-punched nonwoven geotextile made of 100% polypropylene staple fibers, which are formed into a random network for dimensional stability. SKAPS GE-110 resists ultraviolet deterioration, rotting, biological degradation, naturally encountered basics and acids. Polypropylene is stable within a pH range of 2 to 13. SKAPS GE-110 conforms to the physical property values listed below:

| PROPERTY | TEST METHOD | UNIT | M.A.R.V. (Minimum Average Roll Value) |
|---|---|---|---|
| Weight | ASTM D 5261 | oz/sy (g/m$^2$) | 10.0 (339) |
| Thickness* | ASTM D 5199 | mils (mm) | 110 (2.79) |
| Grab Tensile | ASTM D 4632 | lbs (kN) | 270 (1.20) |
| Grab Elongation | ASTM D 4632 | % | 50 |
| Trapezoid Tear Strength | ASTM D 4533 | lbs (kN) | 100 (.44) |
| Puncture Resistance | ASTM D 4833 | lbs (kN) | 165 (.733) |
| Mullen Burst Strength | ASTM D 3786 | psi (kPa) | 525 (3617) |
| Permittivity* | ASTM D 4491 | sec$^{-1}$ | .94 |
| Permeability* | ASTM D 4491 | cm/sec | .30 |
| Water Flow* | ASTM D 4491 | gpm/ft$^2$ (l/min/m$^2$) | 75 (3055) |
| AOS* | ASTM D 4751 | US Sieve (mm) | 100 (.150) |
| UV Resistance | ASTM D 4355 | %/hrs | 70/500 |

* At the time of manufacturing. Handling, storage and shipping may change these properties.

| PACKAGING | |
|---|---|
| Roll Dimensions (W x L) – ft | 15 x 570 |
| Square Yards Per Roll | 950 |
| Estimated Roll Weight - lbs | 620 |

This information is provided for reference purposes only and is not intended as a warranty or guarantee. SKAPS assumes no liability in connection with the use of this information.

SKAPS Industries, 316 S. Holland Dr., Pendergrass, GA 30567, Phone (706) 693-3440, Fax (706) 693-3450, Email: info@skaps.com

**Made in U.S.A.**

Mass: 10 oz/sy = 0.625 lb/sy x 1 sy/9 sf = 0.069 lb/ft2

REFERENCE 2A

REFERENCE 3

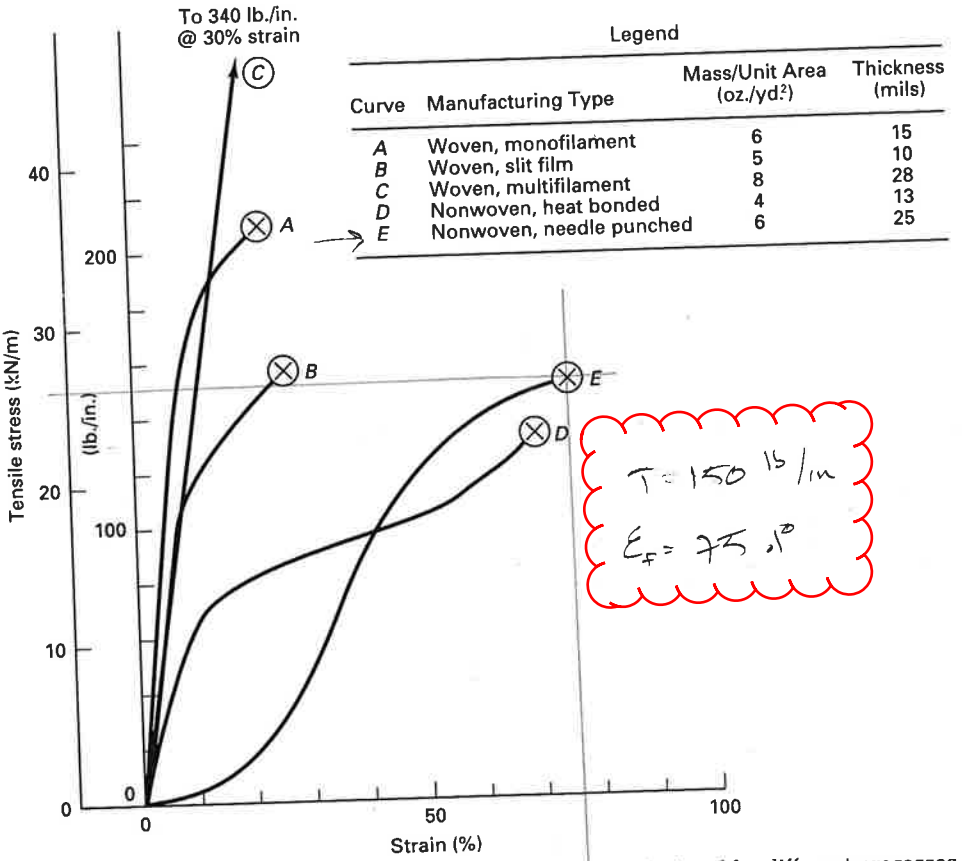


**Figure 2.6** Tensile test response of various geotextiles manufactured by different processes. All are polypropylene fabrics; test specimens were initially 8 in. (200 mm) wide by 4 in. (100 mm) high.

**Solution:** By observation, the strength is

$$T_{max} = 134 \text{ lb./in.}$$

and for 0.013-in. thickness,

$$\sigma_{max} = 10{,}300 \text{ lb./in.}^2$$

The maximum strain is also determined by observation:

$$\epsilon_f = 69\%$$

The toughness ($U$) is then calculated as 1/2 ($T_{max} \times \epsilon_f$) (actually this is an approximation since it should be the area under the curve):

REFERENCE 3

# Skaps Industries, Inc.

Drainage Division
3985 Steve Reynolds Blvd., Bldg. H
Norcross, GA 30093
Phone: (770) 564-1857
Fax: (770) 564-1818

Drainage Product Description Sheet
US Ecology Nevada, Inc.
**TRANSNET 220**

Transnet 220 is a superior quality drainage media made by extruding two sets of HDPE strands together to form a diamond shaped net. This three dimensional structure provides excellent planar liquid flow. The Transnet 220 conforms to the physical property values listed below:

| NET PROPERTY | TEST METHOD | UNITS | M.A.R.V. Minimum Average Roll Value |
|---|---|---|---|
| Weight | ASTM D-5261 | $lbs/ft^2$ | 0.162 ← |
| Thickness | ASTM D-5199 | mils | 220 +/- 20 |
| Density of Polymer | ASTM D-1505 | $g/cm^3$ | 0.940 |
| Tensile Strength | ASTM D-5035 | lbs/in | 45 ← |
| Carbon Black Content | ASTM D-1603 | % | 2 |
| Transmissivity | ASTM D-4716 | $m^2/s$(gpm/sf) | $2 \times 10^{-3}$*(9.66) |
| Melt Flow Index | ASTM D-1238 | g/10min | 1 max |

| | |
|---|---|
| Roll size | 14.5' x 300' |

*Transmissivity measured using water at 20 Degree C (68 degree F) with a gradient of 0.1, under a confining pressure of 10,000 psf, between two steel plates, after 15 minutes. Values may vary based on dimension of the transmissivity specimen and specific laboratory.

The information contained herein has been compiled by Engineered Synthetic Products Inc. and is, to the best of our knowledge, true and accurate. All suggestions or recommendations are offered without guarantee. Final determination of suitability for use based on any information provided, is the sole responsibility of the user. There is no implied or expressed warranty of merchantability or fitness of the product for the contemplated use.

REFERENCE 2B REFERENCE 3

is its thickness, which can be determined using ASTM D1777. While there is no listing as such, it is recommended that geonet thickness be measured under a normal pressure of 420 lb./ft.$^2$ (20 kPa). This is the same pressure that is recommended to measure geomembrane thickness. Geonets are not nearly as sensitive to thickness variation under normal pressure as are geotextiles and are similar to geomembranes in this regard.

Mass per unit area can be determined using ASTM D1910. For a 200-mil (5.1-mm)-thick, extruded, solid-rib geonet, the mass per unit area is usually in the range of 20 to 30 oz./yd.$^2$ (680 to 1020 g/m$^2$). It is not a design property per se, but it is informative from a manufacturer's point of view.

Other physical properties such as rib dimensions, planar angles made by the intersecting ribs, vertical angles made at the juncture locations, aperture size and shape, etc., can be measured directly and are relatively straightforward to obtain.

### 4.1.2 Mechanical Properties

A number of various strength properties of geonets are important to consider.

**4.1.2.1 Tensile Strength** The wide-strip tensile strength of geonets is sometimes called for in various specifications. Using ASTM D4595, which uses a test specimen 8.0 in. (200 mm) in width by 4.0 in. (100 mm) in length, the curves of Figure 4.4 resulted in a 200-mil (5.1-mm)-thick solid rib extruded geonet in the machine and cross-machine directions. Note the differences in behavior, suggesting that there is a preferential direction in strength between the machine and cross-machine directions. If site-specific conditions warrant a high-strength direction, the geonet should be oriented with its machine direction positioned accordingly. Also to be noted is that geonets do indeed possess a measurable tensile strength. For the solid rib geonet illustrated in Figure 4.2 and shown in Figure 4.4, the average of a series of wide-strip tensile tests gave the following information:

- Machine direction:
  Peak strength = 680 lb./ft. (120 kN/m)
  Strain at peak = 23%
  Strain at failure = 290%
- Cross-machine direction:
  Peak strength = 390 lb./ft. (68 kN/m)
  Strain at peak = 170%
  Strain at failure = 240%

**4.1.2.2 Compressive Strength** Of greater importance than the aforementioned in-plane tensile strength of geonets is the cross-plane compressive strength. This is due to the influence that compressive yielding or collapse has on the ability of the geonet to conduct liquid within its planar structure. There are a number of approaches to measuring a geonet's compressive strength, and ASTM has a task committee working on the topic. Using 6.0-in. (150-mm)-square test specimens normally loaded under a constant strain rate load of 0.002 in./min. (= 0.05 mm/

REFERENCE 3

# High Density Polyethylene (Single Sided) Micro Spike® Liner

"80 mil Single Sided Textured"

## Product Data

| Property | Test Method | Values | | |
|---|---|---|---|---|
| Thickness, nominal (mm) | | 60 (1.5) | 80 (2.0) | 100 (2.5) |
| Thickness (min. ave.), mil (mm) | ASTM D5994* | 57 (1.43) | 76 (1.90) | 95 (2.38) |
| Thickness (lowest indiv. for 8 of 10 spec.), mil (mm) | ASTM D5994* | 54 (1.35) | 72 (1.80) | 90 (2.25) |
| Thickness (lowest indiv. for 1 of 10 spec.), mil (mm) | ASTM D5994* | 51 (1.28) | 68 (1.70) | 85 (2.13) |
| *The thickness values may be changed due to project specifications (i.e., absolute minimum thickness) | | | | |
| Asperity Height (min. ave.), mil (mm) | GRI GM12 | 16 (.41) | 16 (.41) | 16 (.41) |
| Density, g/cc, minimum | ASTM D792, Method B | 0.94 | 0.94 | 0.94 |
| Tensile Properties (ave. both directions) | ASTM D6693, Type IV | | | |
| Strength @ Yield (min. ave.), lb/in width (N/mm) | 2 in/minute | 132 (23.1) | 176 (30.8) | 220 (38.5) |
| Elongation @ Yield (min. ave.), % (GL=1.3in) | 5 specimens in each direction | 13 | 13 | 13 |
| Strength @ Break (min. ave.), lb/in width (N/mm) | | 132 (23.1) | 176 (30.8) | 220 (38.5) |
| Elongation @ Break (min. ave.), % (GL=2.0in) | | 350 | 350 | 350 |
| Tear Resistance (min. ave.), lbs. (N) | ASTM D1004 | 45 (200) | 60 (267) | 72 (320) |
| Puncture Resistance (min. ave.), lbs. (N) | ASTM D4833 | 120 (534) | 150 (667) | 180 (801) |
| Carbon Black Content (range in %) | ASTM D4218 | 2 - 3 | 2 - 3 | 2 - 3 |
| Carbon Black Dispersion (Category) | ASTM D5596 | Only near spherical agglomerates for 10 views: 9 views in Cat. 1 or 2, and 1 view in Cat. 3 | | |
| Stress Crack Resistance (Single Point NCTL), hours | ASTM D5397, Appendix | 300 | 300 | 300 |
| Oxidative Induction Time, minutes | ASTM D3895, 200°C, 1 atm $O_2$ | ≥100 | ≥100 | ≥100 |
| Melt Flow Index, g/10 minutes | ASTM D1238, 190°C, 2.16kg | ≤1.0 | ≤1.0 | ≤1.0 |
| Oven Aging | ASTM D5721 | 80 | 80 | 80 |
| with HP OIT, (% retained after 90 days) | ASTM D5885, 150°C, 500psi $O_2$ | | | |
| UV Resistance | GRI GM11 | 20hr. Cycle @ 75°C/4 hr. dark condensation @ 60°C | | |
| with HP OIT, (% retained after 1600 hours) | ASTM D5885, 150°C, 500psi $O_2$ | 50 | 50 | 50 |

**These product specifications meet or exceed GRI's GM13**

## Supply Information (Standard Roll Dimensions)

| Thickness | | Width | | Length | | Area (approx.) | | Weight (average) | |
|---|---|---|---|---|---|---|---|---|---|
| mil | mm | ft | m | ft | m | $ft^2$ | $m^2$ | lbs | kg |
| 60 | 1.5 | 23 | 7 | 410.1 | 125 | 9,419 | 875 | 3,356 | 1,522 |
| 80 | 2.0 | 23 | 7 | 328.1 | 100 | 7,535 | 700 | 3,306 | 1,500 |
| 100 | 2.5 | 23 | 7 | 246.1 | 75 | 5,651 | 525 | 3,167 | 1,436 |

**Notes:**

*All rolls are supplied with two slings. All rolls are wound on a 6 inch core. Special roll lengths are available on request.*

All information, recommendations and suggestions appearing in this literature concerning the use of our products are based upon tests and data believed to be reliable; however, it is the users responsibility to determine the suitability for their own use of the products described herein. Since the actual use by others is beyond our control, no guarantee or warranty of any kind, expressed or implied, is made by Agru/America as to the effects of such use or the results to be obtained, nor does Agru/America assume any liability in connection herewith. Any statement made herein may not be absolutely complete since additional information may be necessary or desirable when particular or exceptional conditions or circumstances exist or because of applicable laws or government regulations. Nothing herein is to be construed as permission or as a recommendation to infringe any patent.

500 Garrison Road, Georgetown, South Carolina 29440 843-546-0600 800-373-2478 Fax: 843-527-2738
email: salesmkg@agruamerica.com www.agruamerica.com

0.94 g/cm3 x (76/1000 inch x 2.54 cm/1 inch) = 0.181 g/cm2 = 0.37 lb/ft2

© Agru America, Inc. 2007

REFERENCE 3

# Skaps Industries, Inc.

3985 Steve Reynolds Blvd.
Norcross, GA 30093
Phone: (770)564-1857
Fax: (770) 564-1818

DRAINAGE PRODUCT DESCRIPTION SHEET

US Ecology Nevada, Inc.

## TRANSNET 220-2-6

Transnet 220-2-6 is a superior quality drainage media made by extruding two sets of HDPE strands together to form a diamond shaped net. The net is then heat laminated to a 6 ounce non-woven fabric. This three dimensional structure provides excellent planar liquid flow. The Transnet 220-2-6 conforms to the physical property values listed below:

| NET PROPERTY | TEST METHOD | UNITS | MINIMUM AVERAGE ROLL VALUE |
|---|---|---|---|
| Mass Per Unit Area | ASTM D-5261 | $lbs/ft^2$ | 0.162 |
| Thickness | ASTM D-5199 | mils | 220 +/- 20 |
| Density of Polymer | ASTM D-1505 | $g/cm^2$ | 0.94 |
| Carbon Black | ASTM D-1603 | % | 2.0 |
| Transmissivity (Geocomposite) | ASTM D-4716 | $Gpm/ft^2$ | 0.48 |
| Tensile Strength | ASTM D-5035 | lbs/in | 50 |
| Ply Adhesion | ASTM 413 | lbs/in | 1.0 |

*Transmissivity of the geocomposite measured using water at 20 Degrees C with a gradient of 0.02, between 2 steel plates, under a confining pressure of 10,000psf, after 15 minutes. Values may vary based on dimension of the transmissivity specimen and specific laboratory.

**STYLE GE-160**

GE-160 is a superior quality, nonwoven geotextile produced by needlepunching together 100% polypropylene staple fibers in a random network to form a high strength dimensionally stable fabric. The polypropylene fibers are specially formulated to resist ultraviolet light deterioration, and are inert to commonly encountered soil chemicals. The fabric will not mildew, is non-biodegradable, and is resistant to damage from insects and rodents. Polypropylene is stable within a ph range of 2 to 13. GE160 conforms to the physical property values below:

| FABRIC PROPERTY | TEST METHOD | UNITS | MINIMUM AVERAGE ROLL VALUE |
|---|---|---|---|
| Weight | ASTM D-5261 | oz | 6.0 |
| Grab Tensile | ASTM D-4632 | lbs | 160 |
| Grab Elongation | ASTM D-4632 | % | 50 |
| Puncture | ASTM D-4833 | lbs | 90 |
| Water Flow Rate | ATMD D-4491 | $gpm/ft^2$ | 110 |
| Permittivity* | ASTM D-4491 | $sec^{-1}$ | 1.5 |
| UV Resistance | ASTM D-4355 | % hours | 70 @ 500 |
| AOS | ASTM D-4751 | US Sieve | 70(max) |

*At time of manufacturing. Handling may change these properties.

To the best of our knowledge the information contained herein is accurate. However, ESP, Inc. cannot anticipate all conditions under which ESP's product information and our products, or the products of other manufacturers in combination with our products, may be used. We accept no responsibility for results obtained by the application of this information or the safety or suitability of our products either alone or in combination with other products. Final determination of the suitability of any information or material for the use contemplated, of its manner of use, and whether the suggested use infringes any patents is the sole responsibility of the user.

Fabric: 6 oz/sy x 1 lb/16 oz x 1 sy/9 sf = 0.042 lb/ft2

Geocomposite = Fabric + Net + Fabric = 0.042 lb/ft2 + 0.162 lb/ft2 + 0.042 lb/ft2 = 0.25 lb/ft2

REFERENCE 3

# High Density Polyethylene Micro Spike® Liner

"60 mil Double Sided Textured"

## Product Data

| Property | Test Method | Values | | | | |
|---|---|---|---|---|---|---|
| Thickness, nominal (mm) | | 30 (.75) | 40 (1.0) | 60 (1.5) | 80 (2.0) | 100 (2.5) |
| Thickness (min. ave.), mil (mm) | ASTM D5994* | 29 (.71) | 38 (.95) | 57 (1.43) | 76 (1.90) | 95 (2.38) |
| Thickness (lowest indiv. for 8 of 10 spec.), mil (mm) | ASTM D5994* | 27 (.68) | 36 (.90) | 54 (1.35) | 72 (1.80) | 90 (2.25) |
| Thickness (lowest indiv. for 1 of 10 spec.), mil (mm) | ASTM D5994* | 26 (.64) | 34 (.85) | 51 (1.28) | 68 (1.70) | 85 (2.13) |
| *The thickness values may be changed due to project specifications (i.e., absolute minimum thickness) | | | | | | |
| Asperity Height (min. ave.), mil (mm) | GRI GM12 | 16 (.41) | 16 (.41) | 16 (.41) | 16 (.41) | 16 (.41) |
| Density, g/cc, minimum | ASTM D792, Method B | 0.94 | 0.94 | 0.94 | 0.94 | 0.94 |
| Tensile Properties (ave. both directions) | ASTM D6693, Type IV | | | | | |
| Strength @ Yield (min. ave.), lb/in width (N/mm) | 2 in/minute | 66 (11.6) | 88 (15.4) | 132 (23.1) | 176 (30.8) | 220 (38.5) |
| Elongation @ Yield (min. ave.), % (GL=1.3in) | 5 specimens in each direction | 13 | 13 | 13 | 13 | 13 |
| Strength @ Break (min. ave.), lb/in width (N/mm) | | 66 (11.6) | 88 (15.4) | 132 (23.1) | 176 (30.8) | 220 (38.5) |
| Elongation @ Break (min. ave.), % (GL=2.0in) | | 350 | 350 | 350 | 350 | 350 |
| Tear Resistance (min. ave.), lbs. (N) | ASTM D1004 | 23 (102) | 30 (133) | 45 (200) | 60 (267) | 72 (320) |
| Puncture Resistance (min. ave.), lbs. (N) | ASTM D4833 | 60 (267) | 90 (400) | 120 (534) | 150 (667) | 180 (801) |
| Carbon Black Content (range in %) | ASTM D4218 | 2 - 3 | 2 - 3 | 2 - 3 | 2 - 3 | 2 - 3 |
| Carbon Black Dispersion (Category) | ASTM D5596 | Only near spherical agglomerates for 10 views: 9 views in Cat. 1 or 2, and 1 view in Cat. 3 | | | | |
| Stress Crack Resistance (Single Point NCTL), hours | ASTM D5397, Appendix | 300 | 300 | 300 | 300 | 300 |
| Oxidative Induction Time, minutes | ASTM D3895, 200°C, 1 atm $O_2$ | ≥100 | ≥100 | ≥100 | ≥100 | ≥100 |
| Melt Flow Index, g/10 minutes | ASTM D1238, 190°C, 2.16kg | ≤1.0 | ≤1.0 | ≤1.0 | ≤1.0 | ≤1.0 |
| Oven Aging | ASTM D5721 | 80 | 80 | 80 | 80 | 80 |
| with HP OIT, (% retained after 90 days) | ASTM D5885, 150°C, 500psi $O_2$ | | | | | |
| UV Resistance | GRI GM11 | 20hr. Cycle @ 75°C/4 hr. dark condensation @ 60°C | | | | |
| with HP OIT, (% retained after 1600 hours) | ASTM D5885, 150°C, 500psi $O_2$ | 50 | 50 | 50 | 50 | 50 |

**These product specifications meet or exceed GRI's GM13**

## Supply Information (Standard Roll Dimensions)

| Thickness | | Width | | Length | | Area (approx.) | | Weight (average) | |
|---|---|---|---|---|---|---|---|---|---|
| mil | mm | ft | m | ft | m | $ft^2$ | $m^2$ | lbs | kg |
| 30 | .75 | 23 | 7 | 600.1 | 182.9 | 13,782 | 1,280 | 3,325 | 1,510 |
| 40 | 1.0 | 23 | 7 | 600.1 | 182.9 | 13,782 | 1,280 | 3,325 | 1,510 |
| 60 | 1.5 | 23 | 7 | 410.1 | 125 | 9,419 | 875 | 3,356 | 1,522 |
| 80 | 2.0 | 23 | 7 | 328.1 | 100 | 7,535 | 700 | 3,306 | 1,500 |
| 100 | 2.5 | 23 | 7 | 246.1 | 75 | 5,651 | 525 | 3,167 | 1,436 |

**Notes:**

*All rolls are supplied with two slings. All rolls are wound on a 6 inch core. Special roll lengths are available on request.*

All information, recommendations and suggestions appearing in this literature concerning the use of our products are based upon tests and data believed to be reliable; however, it is the users responsibility to determine the suitability for their own use of the products described herein. Since the actual use by others is beyond our control, no guarantee or warranty of any kind, expressed or implied, is made by Agru/America as to the effects of such use or the results to be obtained, nor does Agru/America assume any liability in connection herewith. Any statement made herein may not be absolutely complete since additional information may be necessary or desirable when particular or exceptional conditions or circumstances exist or because of applicable laws or government regulations. Nothing herein is to be construed as permission or as a recommendation to infringe any patent.

Executive Offices: 500 Garrison Road, Georgetown, SC 29440 843-546-0600 800-321-1379 Fax: 843-546-0516
email: salesmkg@agruamerica.com

0.94 g/cm3 x (57/1000 inch x 2.54 cm/1 inch) = 0.136 g/cm2 = 0.28 lb/ft2

© Agru America, Inc. 2007

REFERENCE 3

# GEOSYNTHETIC CLAY LINERS

| Product Name | Bonding Method | Needlepunched Peel Strength ASTM D6496, N/m (lb/in) | GCL Dimensional Properties | | | GCL Hydraulic Properties | Base Bentonite Properties | | GCL Structural Components | | | | Manufacturer's Suggested Applications [3] |
|---|---|---|---|---|---|---|---|---|---|---|---|---|---|
| | | | | | | | | | Upper Geosynthetic | | Lower Geosynthetic | | |
| | | | Panel Size Roll Width/ Length m/m (ft/ft) | Average Roll Weight kg (lb) | Bentonite Mass/Unit Area ASTM D5993 gm/m2 (lb/ft2) | Flux [1] ASTM D 5887 [2] m3/m2-s | Swell Index ASTM D 5890 (min) ml/2g | Fluid Loss ASTM D 5891 ml | Type or structure | Weight ASTM D5261 or Thickness ASTM D5199 g/m2 or mm (oz/yd2 or mil) | Type or structure | Weight ASTM D5261 or Thickness ASTM D5199 g/m2 or mm (oz/yd2 or mil) | |
| **CETCO Lining Technologies \| www.cetco.com** | | | | | | | | | | | | | |
| Bentomat 600CL | needlepunched laminated | 175 (1.0) | 4.6/45.7 (15/150) | 1250 (2750) | 3660 (0.75) | 1 x 10-9 | 24 | 18 | FML/geotextile composite | NA | woven | 105 (3.2) | LL, LC, SIC, CL, SIL |
| Bentomat CL | needlepunched laminated | 610 (3.5) | 4.6/45.7 (15/150) | 1250 (2750) | 3660 (0.75) | 1 x 10-9 | 24 | 18 | FML/geotextile composite | NA | woven | 105 (3.2) | LL, LC, SIC, CL, SIL |
| Bentomat CLT | needlepunched laminated | 610 (3.5) | 4.6/45.7 (15/150) | 1340 (2950) | 3660 (0.75) | 1 x 10-9 | 24 | 18 | textured FML/ geotextile composite | 0.5 (20) | woven | 105 (3.2) | LL, LC, SIC, CL, SIL |
| Bentomat DN | needlepunched | 610 (3.5) | 4.4/45.7 (14.5/150) | 1220 (2700) | 3660 (0.75) | 1 x 10-8 | 24 | 18 | nonwoven | 200 (6.0) | nonwoven | 200 (6.0) | LL, LC, SIC |
| Bentomat SDN | needlepunched | 525 (3.0) | 4.4/45.7 (14.5/150) | 1200 (2650) | 3660 (0.75) | 1 x 10-8 | 24 | 18 | nonwoven | 200 (6.0) | nonwoven | 90 (2.7) | LL, LC, SIC |
| Bentomat ST | needlepunched | 610 (3.5) | 4.6/45.7 (15/150) | 1200 (2650) | 3660 (0.75) | 1 x 10-8 | 24 | 18 | nonwoven | 200 (6.0) | woven | 105 (3.2) | LL, LC, SIC |
| Bentomat STM | needlepunched | 610 (3.5) | 4.6/60.9 (15/200) | 1133 (2500) | 2440 (0.50) | 3 x 10-8 | 24 | 18 | nonwoven | 200 (6.0) | woven | 105 (3.2) | LL, LC, SIC |
| Bentomat 200R | needlepunched | 175 (1.0) | 4.6/45.7 (15/150) | 1200 (2650) | 3660 (0.75) | 1 x 10-8 | 24 | 18 | nonwoven | 105 (3.2) | woven | 105 (3.2) | LL, LC, SIC |
| **GSE Lining Technology Inc. \| www.gseworld.com** | | | | | | | | | | | | | |
| GSE BentoLiner CNSL | needlepunched, polymer-coated | 610 (3.5) | 4.7/46 (15.5/150) | 1180 (2600) | 3660 (0.75) | 1 x 10-9 | 24 | 18 | nonwoven | 200 (6.0) | PP geofilm/ woven composite | 105 (3.1) | high head applications with low hydraulic conductivity |
| GSE BentoLiner EC | needlepunched | 175 (1.0) | 4.7/46 (15.5/150) | 1180 (2600) | 3660 (0.75) | 1 x 10-8 | 24 | 18 | nonwoven | 100 (3.0) | woven | 105 (3.1) | Low Loads and Flat Slopes |
| GSE BentoLiner NSL | needlepunched | 610 (3.5) | 4.7/46 (15.5/150) | 1180 (2600) | 3660 (0.75) | 1 x 10-8 | 24 | 18 | nonwoven | 200 (6.0) | woven | 105 (3.1) | Medium Loads and Slopes |
| GSE BentoLiner NWL | needlepunched | 610 (3.5) | 4.7/46 (15.5/150) | 1180 (2600) | 3660 (0.75) | 1 x 10-8 | 24 | 18 | nonwoven | 200 (6.0) | nonwoven/ woven composite | 200 (6.0) | Medium Loads and Slopes |
| GSE BentoLiner NWL-35 | needlepunched | 928 (5.3) | 4.7/46 (15.5/150) | 1180 (2600) | 3660 (0.75) | 1 x 10-8 | 24 | 18 | nonwoven | 200 (6.0) | nonwoven/ woven composite | 200 (6.0) | High Loads and Steep Slopes |
| GSE BentoLiner NWL-60 | needlepunched | 2,100 (12.0) | 4.7/46 (15.5/150) | 1180 (2600) | 3660 (0.75) | 1 x 10-8 | 24 | 18 | nonwoven | 200 (6.0) | nonwoven/ woven composite | 200 (6.0) | Very High Loads and Steep Slopes |
| GSE BentoLiner EC-CAR | needlepunched polymer enhanced | 175 (1.0) | 4.7/46 (15.5/150) | 1180 (2600) | 3660 (0.75) | 1 x 10-8 | 24 | 18 | nonwoven | 100 (3.0) | woven | 105 (3.1) | Coal Ash Resistant |
| GSE BentoLiner NSL-CAR | needlepunched polymer enhanced | 610 (3.5) | 4.7/46 (15.5/150) | 1180 (2600) | 3660 (0.75) | 1 x 10-8 | 24 | 18 | nonwoven | 200 (6.0) | woven | 105 (3.1) | Coal Ash Resistant |

[1] Flux is defined as "Flow rate/unit area" which can be converted to permeabilitly using the equation: Permeability = flux/hydraulic gradient

[2] Report result at a maximum confining stress of 35 kPa (5 psi) and 14 kPa (2 psi) head pressure

[3] CL = Canal liner
LL = Landfill liner
SIC = Surface impoundment cover
LC = Landfill cover
SIL = Surface impoundment liner

NP = Not provided by manufacturer
NA = Not applicable, per manufacturer

Companies were requested to provide minimum roll values (MARV). All claims are the responsibility of the manufacturer.

« *Geosynthetics* recommends you contact the manufacturers before making any specifying/purchasing decisions »

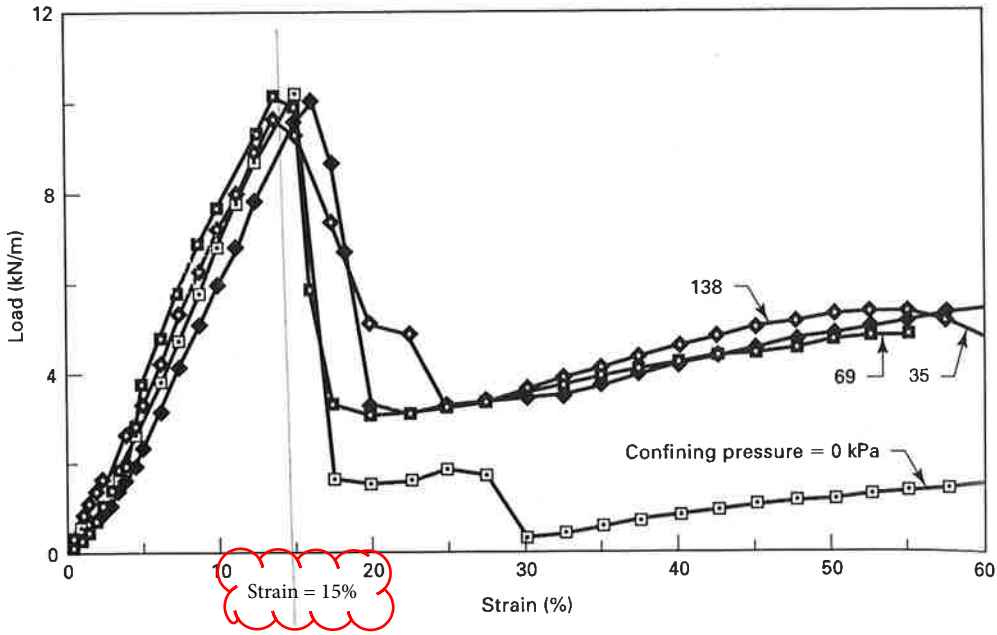


(a) Load-extension behavior of GCL A

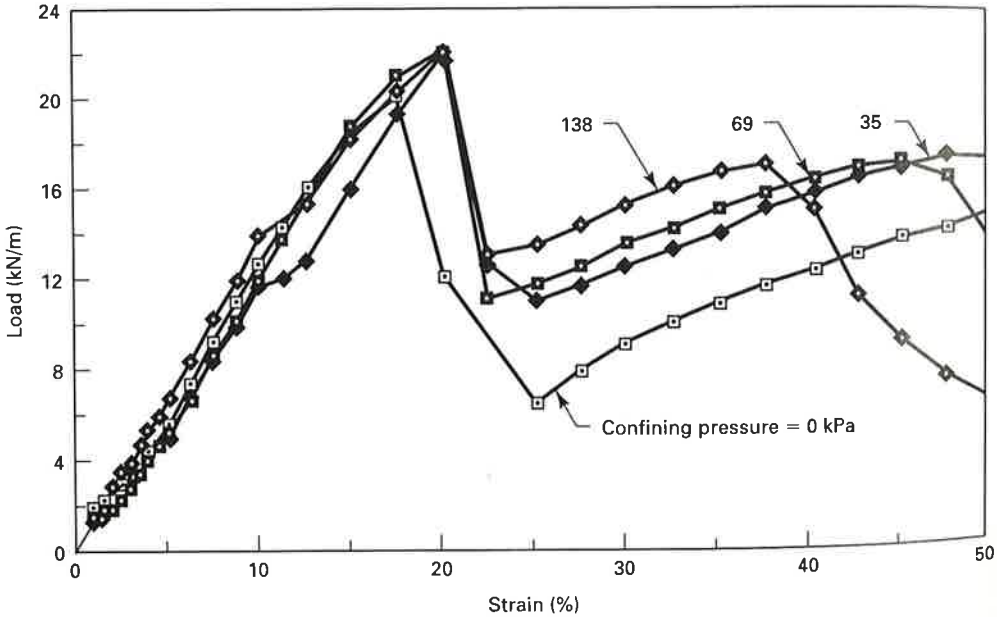


(b) Load-extension behavior of GCL B

**Figure 6.5** Wide-width tensile behavior of two GCLs per ASTM test method D4595 (modified).

REFERENCE 3

## PRODUCT CERTIFICATIONS

PROJECT NAME: US Ecology Trench 12
CUSTOMER P.O.: 13006
ORDER NUMBERS: 000291050
PREPARED FOR: EC Applications

The GCL manufactured for the above-referenced order number(s) is certified to meet the values listed in the tables below:

### GCL PROPERTY SPECIFICATIONS FOR BENTOMAT DN

| Test Method | Test Method Property | Test Frequency | Certified Value |
|---|---|---|---|
| ASTM D 5891 | Bentonite Fluid Loss | 1 per 50 Tons | 18 ml Max |
| ASTM D 5993 | Bentonite Mass/Area | 40,000 sq ft (4000 sq m) | 0.75 lb /sq ft Min |
| ASTM D 5890 | Bentonite Swell Index | 1 per 50 Tons | 24 ml/2g Min |
| ASTM D 6768 | GCL Grab Strength | 200,000 sq ft (20,000 sq m) | 50 lbs/in MARV |
| ASTM D 6243 | GCL Hydrated Internal Shear Strength | Periodic | 500 psf typ @ 200 psf normal load |
| ASTM D 5887 | GCL Hydraulic Conductivity | Weekly | 5.0E-9 cm/s Max |
| ASTM D 5887 | GCL Index Flux | Weekly | 1.0E-8 m3/m2/s Max |
| ASTM D 6496 | GCL Peel Strength | 40,000 sq ft (4000 sq m) | 3.5 lbs/in Min |

Bentonite property tests are performed at a bentonite processing facility before shipment to CETCO's production facility. All tensile testing is in the machine direction using ASTM D 6768. All peel strength testing is performed using ASTM D 6496. Upon request tensile and peel results can be reported per modified ASTM D 4632 using 4 inch grips.

## NEEDLE DETECTION AND REMOVAL PROCEDURE

CETCO hereby affirms that all Bentomat® geosynthetic clay liner material manufactured for this project is continually passed under a magnet for needle removal and then screened with a metal detection device. CETCO certifies Bentomat® to be essentially free of broken needles and fragments of needles that would negatively effect the performance of the final product.

Roger B. Wilkerson
Quality Assurance Coordinator